UNIVERSITY OF TROMSØ UIT

FACULTY OF HEALTH SCIENCES
DEPARTMENT OF MEDICAL BIOLOGY

UNIVERSITY HOSPITAL OF NORTH NORWAY
DEPARTMENT OF MICROBIOLOGY AND INFECTION CONTROL
REFERENCE CENTRE FOR DETECTION OF ANTIMICROBIAL RESISTANCE

THE NORWEGIAN STRUCTURAL BIOLOGY CENTRE (NorStruct)
DEPARTMENT OF CHEMISTRY

Structural and biochemical investigation of Metallo-β-lactamases; Insights into the antibiotic binding sites

Borra. Naga Pardha Saradhi

A dissertation for the degree of
Philosophiae Doctor

June 2012

Acknowledgement

The present work has been carried out in the period of January 2009 to May 2012 at the Research Group of Host-Microbe Interactions, University of Tromso (UIT), and Reference Centre for Detection of Antimicrobial Resistance (K-res), and The Norwegian Structural Biology Centre (NorStruct), University of Tromso. The financial support for this study was provided from University of Tromso, Tromso Research Foundation, and Northern Norway Regional Health Authority.

First and foremost I sincerely would like to thank my main supervisor Ørjan Samuelsen for giving me an opportunity, and accepting me as a PhD student. I am really grateful for his guidance, support, patience, enthusiasm, and knowledge, without which this work could have not been completed. You are always cooperative, all the time your door was opened for me, and really helped me a lot with your excellent guidance and knowledge. I am really thankful to my co-supervisor Hanna-Kirsti S. Leiros for her support, patience and knowledge. You are the one introduced the great field of Structural Biology to me and whatever I have learnt is because of your support and guidance. You never discouraged me, and always encouraged me during the discussions and learning process of structural biology. I am thankful and grateful to my co-supervisor Professor Arnfinn Sundsfjord for the opportunity given to me to come to Norway, and work with this wonderful group. Without your support I would have not been in Norway to take up PhD. You are very kind and supportive from my first day in Tromso and gave morale support during my difficult periods. Special thanks to my collaborators Professor Timothy R. Walsh and Dr. James Spencer. Thanks to all co-authors on the submitted and prepared manuscripts.

Thanks to fellow researchers and colleagues at Host-Microbe Interactions, K-res, and NorStruct departments for providing me media, materials, methods, and nice working environment. Special thanks to Trine, Tove and Stephen. Special thanks to Bettina, Bjørg, Elizabeth and Belinda.

I thank Professor Umesh Varshney from IISc for the opportunity given for me to introduce to the research field and thanks to my colleagues in IISc for wonderful research days we spent in IISc campus. I take this opportunity to thank my lecturers K.J.R Kishore, A. Srinivasa Rao and Kiranmayee.

I am truly thankful to Umaer and family, Anoop and Anupama for the support all the time. I am really thankful to my friends Krishna Madhu and Hemanth for their friendship. Special thanks to Dr. Khaled for the help during my difficult time.

Last but not least, a humble and respectable appreciation to my family back home in India for their support and affection. I am forever thankful to my wife Dhivya, stood all the time my side during difficult periods, and without your support and you, I would have not be a happy man and finish this PhD. Love for my lovely son Saathvik for cheering me after hard days at work with his beautiful smile. I am really grateful to my grand father Seshaiah, being on my side all the time, without his support I would have not perused higher studies. I would like to dedicate my PhD to my grand father Sri. Seshaiah.

Borra. Naga Pardha Saradhi
Tromsø, June 2012

Table of Content

Definitions & Abbreviations:

Helix:	A twisted shape structure like spring.
Motif:	A recurring pattern of amino acid in a sequence
MBL:	Metallo-β-lactamase
ESBL:	Extended Spectrum β-lactamase
IS*CR*:	Insertion sequence common region
OMP:	Outer membrane porin
BBL numbering:	Class B β-lactamase standard numbering
EDTA:	Ethylenediaminetetraacetic acid
CA:	Clavulanic acid
E-S:	Expanded-Spectrum
Zn^{2+}:	Zinc ion
Zn1:	First zinc
Zn2:	Second zinc
PBP:	Penicillin binding protein
MurNAc or NAM:	*N*-acetylmuramic acid
GlcNAc or NAG:	*N*-acetyl glucosamine
IMPs:	Imipenemase
VIMs:	Verona Imipenemase
NDMs:	New Delhi Metallo-β-lactamase
GIM-1:	German Imipenemase-1
AIM-1:	Adelide Imipenemase-1
PDB:	Protein Data Bank
MRSA:	Methicillin resistant *Staphylococcus aureus*
VLS:	Virtual Ligand Screening
MIC:	Minimum inhibitory concentration

1. Introduction

1.1 Antibiotics:

The term “antibiotic” was given by Selman Waksman in 1942 to substances produced by microorganisms that inhibit the growth of other microorganisms [1]. However, today the term antibiotic is used for substances or antimicrobial agents from natural or synthetic sources (any class of organic molecule), that kill or inhibit the growth of microbes by specific interactions with bacterial targets, without harming the eukaryotic host harboring the infecting bacteria [2, 3]. An antimicrobial agent must have the potency (enter into the bacterium cell) and access (should be able to reach the target) in order to exert its antimicrobial action [4]. The major classes of antibiotics inhibit or kill the bacteria mainly by targeting a) cell-wall biosynthesis, b) protein synthesis, c) DNA replication and repair, d) disruption of bacterial membrane, and e) folic acid synthesis [3, 5] (Table 1).

Table 1: Classification of antimicrobials based on their target site (modified from Tenover, F C, 2006) [6].

Target site	Target	Antibiotic
Inhibition of cell wall synthesis	Penicillin binding proteins, D-alanyl-D-alanine, Muropeptide transport	Penicillins, Cephalosporins, Carbapenems, Monobactams, Daptomycin, Glycopeptides
Inhibition of protein synthesis	30s and 50s subunits of the ribosome	Tetracyclines, Chloramphenicol, Macrolides, Aminoglycosides, Lincosamides, Oxazolidinones, Streptogramins
Interference of nucleic acid synthesis	DNA gyrase, DNA structure integrity, RNA polymerase	Quinolones, Nitroimidazoles, Rifampicin
Disruption of bacterial membrane	Phospholipid structure	Polymixins
Inhibition of folic acid pathway	Dihydrofolate reductase, Dihydropteroate synthetase	Sulphonamides, Trimethoprim

1.2 Antibiotic resistance and mechanisms:

Antibiotic resistance can be defined as “the ability of a microorganism to resist the antibiotic pressure and survive” [3, 7], in contrast to the susceptible bacteria which will be eliminated. The effect of an antibiotic can either be bacteriostatic or bactericidal based upon the antibiotic target and concentration. Bacterial susceptibility to a particular antibiotic can be defined from both a microbial and a clinical point of view [8]. From a bacterial point of view, a susceptible bacterium belongs to a sub-population lacking mechanisms of resistance [8]. Such susceptible bacteria may develop resistance by acquiring antibiotic resistance genes or mutations, and hence being able to survive antibiotic exposure, and become resistant [8]. From a clinical point of view, when the bacterium responds to antibiotic therapy it is termed susceptible, and if the bacteria does not respond to antibiotic therapy it is categorized as resistant to that particular antibiotic. Therefore clinically, bacteria can be divided into susceptible, intermediate susceptible, or resistant to antibiotics [8]. Mechanisms of resistance are found within bacteria either intrinsically or they may be acquired. The intrinsic resistance refers to existence of resistance genes as part of the genome encoding mechanisms intrinsically found in the population of the bacteria (genus or species) [2]. For instance, Gram-negative bacteria are intrinsically resistant to glycopeptides and macrolides due to their impermeable outer membrane [9]. Further, due to the lack of a cell-wall, *Mycoplasma* intrinsically shows resistance to β-lactams and other cell-wall biosynthesis targeting antibiotics [9]. In contrast, the acquired resistance mechanisms are attained by bacteria through mutations or mechanisms of horizontal gene transfer such as transformation, conjugation, and transduction [10, 11]. For instance, many β-lactamase genes are acquired by bacteria through mobile genetic elements such as plasmids [12-14], transposons [15], and insertion sequence common region (IS*CR*) elements [16]. Plasmids can replicate independently within bacteria and also transfer between bacterial cells and species, spreading resistance [3, 13]. Further, the rapid generation time of

bacteria assist them to evolve quickly and hence become resistant to antibiotics with in a short period of time [10].

Generally bacteria exhibits biochemical resistance by three different mechanisms (Figure 1); a) by reducing their permeability into the cell and/or by active efflux mechanism [17, 18], b) by structurally altering the antibiotic targets [19], c) by enzymatic modification or inactivation of the antibiotic before reaching the targets [4, 20]. Bacteria can combine these mechanisms to exhibit resistance towards antibiotics [21].

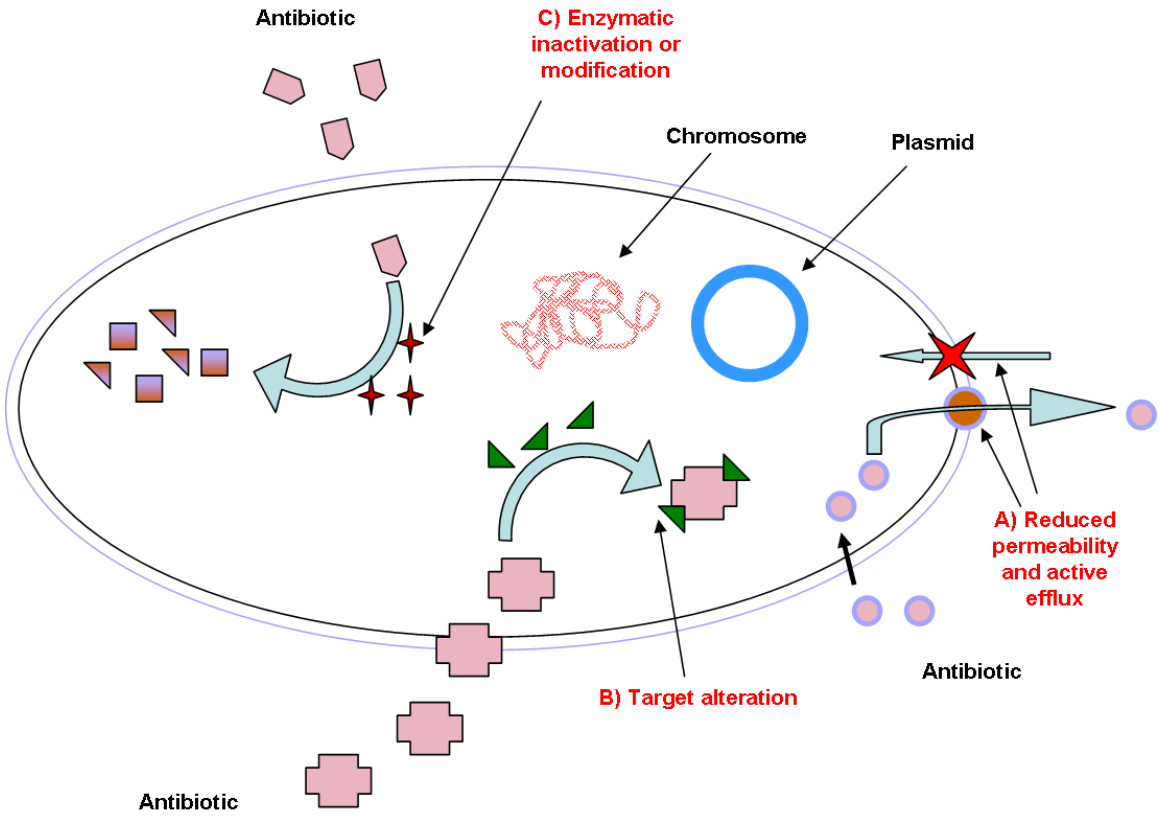

Figure 1: An overall representation of bacterial resistance mechanisms (modified from Levy, S.B et al., 2004) [5].

A brief overview of the different mechanisms will be given below with the main focus on resistance to β-lactams. A more detailed description of β-lactamases will be discussed later.

1.2.1 Reduced permeability and active efflux:

In Gram-negative bacteria, the outer membrane contains protein channels, formed by porin proteins important for nutrient transportation into the cell [22]. In order to prevent the entry of antibiotics, bacteria reduce the access of antibiotics mainly by changing the outer membrane (in Gram-negative bacteria) and cell wall (in Gram-positive bacteria). Gram-negative pathogens like *Klebsiella pneumoniae, Pseudomonas aeruginosa*, and *Acinetobacter baumannii* show resistance to antibiotics like β-lactams by altering the porins or by loss of porins [23]. As an example, the combination of deletion of outer membrane porins with the production of plasmid-mediated AmpC β-lactamases in *K. pneumoniae* can confer resistance to imipenem [24]. Another strategy is expelling the antibiotics out of the bacterial cell by active efflux through membrane bound efflux pumps [18]. *P. aeruginosa* harbour several efflux pumps like MexAB-OprM, MexCD-OprJ, and MexXY-OprM with various spectre of substrate profiles that includes different groups of antibiotics including β-lactams [25].

1.2.2 Target alteration:

Bacteria can alter the targets of antibiotics structurally reducing the affinity for antibiotics. For instance, modification of penicillin binding proteins (PBPs) which are the main targets for β-lactams reduces the affinity for β-lactams [26]. The most known example is methicillin resistant *Staphylococcus aureus* (MRSA) which is achieved by the acquisition of an altered PBP (PBP2a or PBP2') by the *mecA* gene [27]. Also in Gram-negative bacteria such as *A. baumannii* [28] and *P. aeruginosa* [29] altered PBPs have been implicated in resistance towards β-lactams.

1.2.3 Enzymatic inactivation or modification:

Most of the antibiotics are characterized by ester or amide bonds, which are hydrolytically susceptible, targeted by certain bacterial enzymes, and render them inactive [30]. β-lactamases are the major resistance mechanisms in this respect (discussed later). Modification of the antibiotic molecule is a major resistance mechanism in Gram-negatives to aminoglycosides conferred by aminoglycoside modifying enzymes [31].

1.3 β-Lactam antibiotics:

The first antibiotic was accidentally discovered by Sir Alexander Fleming in 1928 from a mould culture of *Penicillium notatum*, which was able to kill *Staphylococci* [14]. The active substance from *Penicillium* was named “penicillin” [32]. Howard Florey and Ernst Boris Chain were able to produce penicillin in large quantities [33], which was first used to treat bacterial infections during the Second World War saving many lives and penicillin became known as the “magic bullet”. The discovery of penicillin revolutionized treatment of infectious diseases and became a milestone for the modern medicine. Fleming, Florey and Chain were awarded the Nobel Prize of Medicine and Physiology in 1945 for the discovery and application of penicillin. Later in 1949 the structure of penicillin was solved by x-ray crystallography and the β-lactam ring of penicillin was indentified as the key functional property [34]. Since the discovery of penicillin, β-lactams have been our most important antibiotic group (>65% worldwide market) for the past 70 years and are used to treat infections caused by both Gram-negative and Gram-positive bacteria [17, 35]. Based on the structure and discovery, β-lactams can be classified into four major groups; penicillins, cephalosporins, carbapenems, and monobactams (Figure 2).

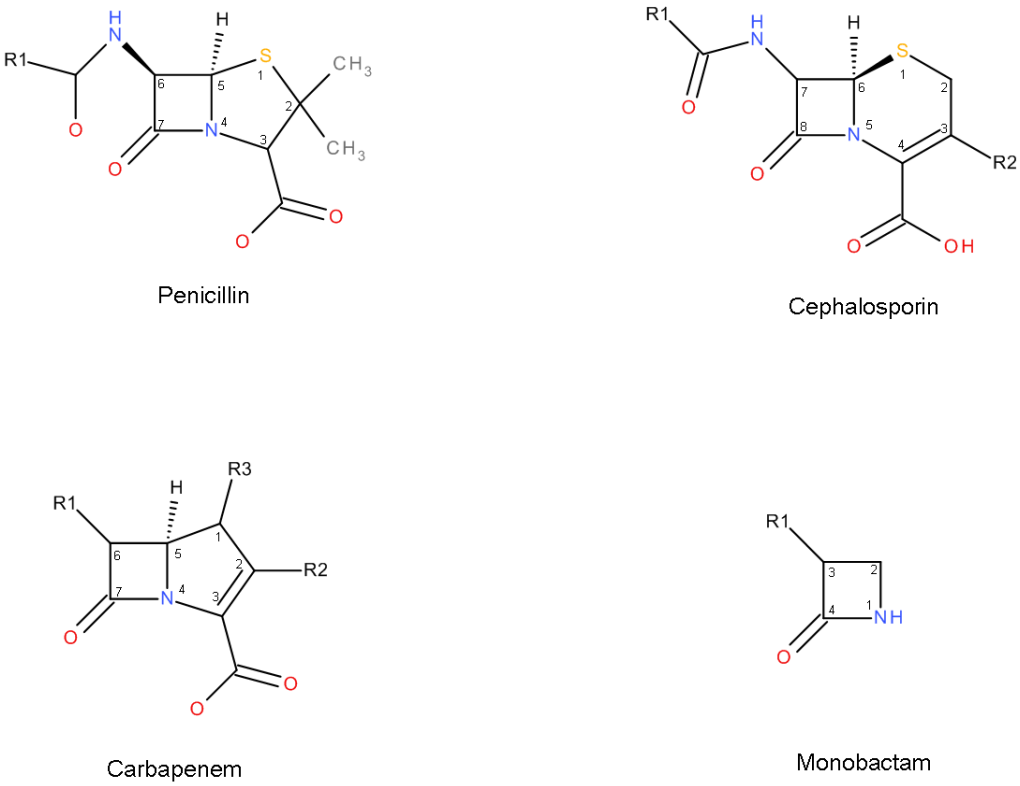

Figure 2: The core structures of β-lactams. The figure is generated by Accelrys Draw.

The β-lactams are either natural or semisynthetic molecules, characterized by a basic nucleus of a four-membered lactam ring containing three carbon atoms and one nitrogen atom. In further development, the β-lactam ring is fused with a five or six membered ring in a bicyclic ring structure to enhance biological activity, β-lactamase stability, and reduce toxicity [17, 36]. The β-lactam ring is fused with a five-membered thiazolidine ring for penicillins, and to a six-membered dihydrothiazine ring for cephalosporins. Carbapenems have an additional ring that is similar to that of penicillins but is unsaturated and the sulphur atom is substituted by a carbon atom. In contrast, monobactams have no fused structures to the β-lactam ring. Further, different β-lactams belonging to same

group are distinguishable by their side chain groups (such as R1, R2 and possibly R3) [36].
The four different classes of β-lactam antibiotics are described below in brief.

Penicillins:

Penicillins have low toxicity to the host and generally show high activity against the Gram-positive bacteria. In general, the basic structure of penicillins contains a thiazolidine nucleus attached to the β-lactam ring, and a side chain at the C6 position [34]. The side chain represents different groups of penicillins; penicillin G (group 1), penicillin M (group 2), penicillin A (group 3), 6-α-substituted penicillins (group 4), α-carboxy- and α-sulfopenicillins (group 5), amidinipenicillins (group 6), and oxyiminopenicillins (group 7) [37].

Cephalosporins:

The first cephalosporin was discovered from a fungal culture filtrate of *Cephalosporium acremonium* in 1945 and from a mutant culture of *C. acremonium,* 7-aminocephalosporanic acid (cephalosporin-C) were produced in large quantities [38]. Cephalothin, a chemically modified cephalosporin-C, was the first cephalosporin issued for parental use [39]. Cephalosporins core structure contains the β-lactam ring fused to a six-membered dihydrothiazine ring, with a sulphur atom at position 1 [39]. Cephalosporins are generally classified based on the antimicrobial activity and historical development into four generations. Each newer generation has significant greater activity towards Gram-negative bacteria than previous generation [17]. 1st generation cephalosporins (e.g. cefazolin, cephaloridine, and cephalothin) have better activity on Gram-positive than Gram-negative bacteria. 2nd generation cephalosporins (e.g. cefoxitin, cefuroxime and ceftriaxone) have increased Gram-negative activity whilst retaining some Gram-positive activity and are more resistant to β-lactamases. The 3rd generations (e.g. ceftazidime, cefotaxime, and cefixime) with some exceptions, have better Gram-

negative activity towards *Enterobacteriaceae* with less Gram-positive activity. The 4th generation (e.g. cefepime, cefpirome, and cefozopran) exhibit high activity on both Gram-positive and Gram-negative bacteria. Further, 4th generation cephalosporins are more stable against β-lactamases, and have enhanced ability to cross through porins in the outer membrane. Based on the chemical structure, cephalosporins can be classified into six groups; α-amino cephalosporins based on the C3 side chain such as cefadroxil (group 1; cephaloglycin and group 2; ceftrizine), miscellaneous derivatives such as ceftibuten (group 3), oral cephalosporin prodrugs such as cefuroxime (group 4), aryloxyimino derivative nonesterified compounds such as cefixime (group 5), and carbacephems such as loracarbef (group 6) [39].

The cephamycins are structurally similar to cephalosporins, but the cephalosporin nucleus is fused with a 7-alpha-methoxyl group. The additional group gives high level resistance to class A β-lactamases [17]. Cephamycins are produced from *actinomycetes.* The first semisynthetic cephamycins was cefoxitin.

Carbapenems:

The first carbapenem discovered was thienamycin from the culture filtrate of *Streptomyces cattleya* [40-42]. Thienamycin was unstable at pH >8, and thus was not suitable for clinical use [41]. Carbapenems can be divided into either natural origin such as thienamycin, or synthetic origin such as imipenem. Imipenem (*N*-formimidoyl thienamycin is a chemically stable compound compared to thienamycin, and was the first carbapenem approved for clinical use [43, 44]. The basic structure of carbapenems contains a four member β-lactam ring fused to a five member thiazolidinic secondary ring through the nitrogen and adjacent tetrahedral carbon atom [45]. The side chains fused to the core structure influence the antimicrobial activity [45, 46]. Carbapenems are the most potent class of β-lactams, and exhibits high activity against Gram-positive, Gram-negative, and anaerobic bacteria [45, 47]. Imipenem has a non-substituted group

at position 1 to the basic thienamycin nucleus. Meropenem is structurally different with a methyl group. Other carbapenems approved for clinical use includes ertapenem and doripenem [45, 48].

Monobactams:

SQ-26180 was the first monocyclic β-lactam derived naturally from *Chromobacterium violaceum* [49]. Later, this compound was successfully developed by in 1985 by demethoxylation at the C3 position and substitution with a 2-amino-5-thiazolyl oxime moiety into aztreonam [50]. Aztreonam is the only monobactam in clinical use and show high activity against *Enterobacteriaceae* and good efficacy against *P. aeruginosa* [51]. An overview of the antibacterial spectrum of β-lactams is presented in Table 2.

Table 2: Classes of β-lactams and the antibacterial spectrum (modified from online text book of bacteriology by Kenneth, Todar [52].

β-lactam	Chemical class	Examples	Spectrum of activity	
			Gram-positive	Gram-negative
Penicillins	Penicillins	Penicillin-G, Penicillin-M	+	-
	Semi-synthetic β-lactams	Amoxicillin, Ampicillin	+	+
Cephalosporins	1st generation	Cephalothin, Cefazolin	+	±
	2nd generation	Cefoxitin, Cefuroxime	±	+
	3rd generation	Ceftazidime, Cefotaxime	±	+
	4th generation	Cefepime, Cefpirome	+	+
Penems	Carbapenems	Imipenem, Meropenem	+	+
Monobactams	Monobactams	Aztreonam	+	+

+: good activity; ±: reduced activity.

1.3.1 Mechanism of action of β-lactams:

The β-lactams exert their bactericidal activity primarily on the cell-wall biosynthesis in bacteria. In the 1960s, the structure of the bacterial cell wall and the mechanism of its biosynthesis were described [53, 54]. The cell wall is a protective barrier for the bacterium in order to maintain the rigidity and to resist the internal osmotic pressure, and participates in cell division [55]. The bacterial cell wall is mainly composed of peptidoglycan; a complex polymer consisting of linear glycans interlinked by peptide chains and sugars, responsible for shape and integrity of the cell wall [53, 56]. The glycans chains are composed of alternating units of *N*-acetylmuramic acid (MurNAc or NAM) and *N*-acetyl glucosamine (GlcNAc or NAG), which are linked to sugars by β-1-4 glycosidic bonds [56]. The neighbouring glycan subunits are interlinked either by direct linkage between peptide subunits of one chain with other peptide chains or by a short (5 amino acid long) peptide bridge between two peptides [56] to form a rigid network (Figure 3).

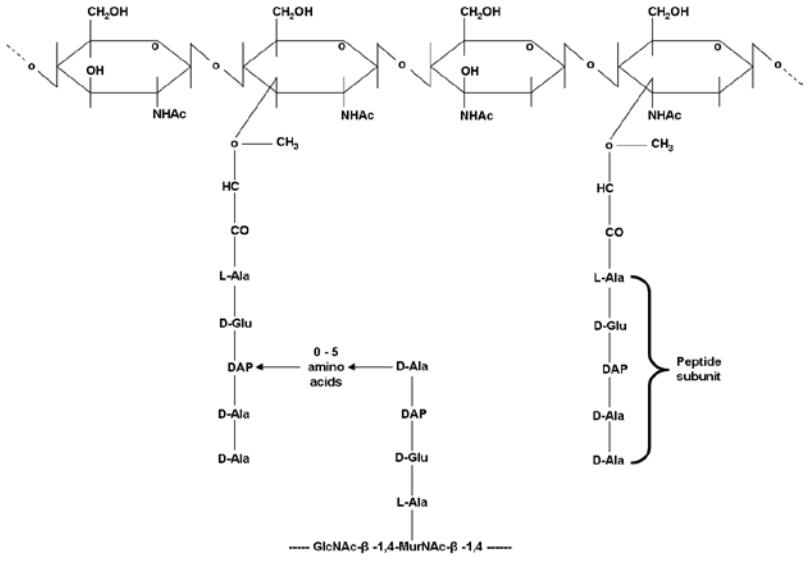

Figure 3: Bacterial peptidoglycan structure. (MurNAc: N-acetylmuramic acid; GlcNAc: N-acetyl glucosamine; DAP: Diaminopimelic acid or L-lysine). Modified from Van Heijenoort J, 2001 [56].

The cell wall biosynthesis is performed by a series of membrane located transpeptidase enzymes, penicillin binding proteins (PBPs), due to their ability to bind penicillin molecules [26, 57, 58]. PBPs involved in peptidoglycan synthesis include activities such as glycosyltransferase, transpeptidase, and carboxypeptidase activities and are responsible for the cross-linking between the peptidoglycan subunits [19]. Many variants of PBPs are described (PBP1, PBP2, PBP2A, PBP2B, PBP3-PBP6), and categorized as low and high molecular weight PBPs [59]. In general, β-lactams target the cell wall biosynthesis by binding and inhibiting the PBP. The β-lactam nucleus mimics the terminal D-alanyl-D-alanine residue of the peptide and interfere with the serine hydroxyl group of PBPs inhibiting the transpeptidation reaction [60].

1.4 β-lactamases:

The effectiveness of β-lactams relies upon their accessibility to their targets (PBP) and ability to inhibit them. The most common mechanism of resistance to β-lactams in bacteria is the production of hydrolytic enzymes, termed β-lactamases, which inactivates the β-lactams by disrupting the amide bond of their β-lactam ring [17, 35]. In Gram-positive bacteria, β-lactamses are either bound to the cytoplasmic membrane or excreted into the extracellular space, whereas in Gram-negative bacteria they are located in the periplasmic space [4]. β-lactamses are structurally related to PBPs and it is suggested that they might have evolved from the β-lactam binding enzymes of the cell wall biosynthesis [57]. The first β-lactamase was reported in *Escherichia coli* in 1940 [61], before the clinical release of penicillin. Since then β-lactamases have been reported in Gram-positive, Gram-negative bacteria and mycobacteria [62, 63]. So far more than 1000 β-lactamases have been reported (Figure 4) [2, 64]. These enzymes are either chromosomally encoded or the genes are located on mobile genetic elements such as plasmids or transposons [65]. Consequently, bacteria are able to acquire β-lactamase genes and become resistant to β-lactams.

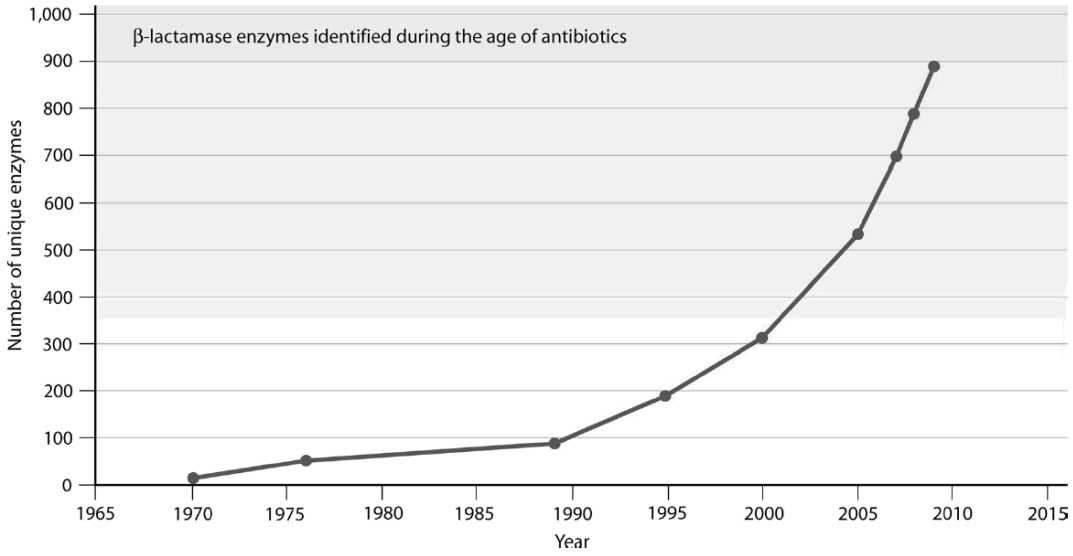

Figure 4: Diagrammatic representation of number of β-lactamses reported since 1970 [2].

1.4.1 Classification of β-lactamses:

β-lactamases show great diversity and different schemes have been proposed to classify them based on functional and biochemical properties [10, 66], as well as amino acid sequence similarities [67]. In the Ambler molecular classification scheme β-lactamases are classified into four different molecular classes, class A, B, C, and D based on amino acid sequence criteria (Table 3) [67]. The Ambler molecular classification can be grouped structurally into two super families; serine β-lactamses (class A, B, and D) and metallo-β-lactamses (class B). Although, serine β-lactamses and metallo-β-lactamses hydrolyze the β-lactams, the catalytic mechanism is notably different between them. The serine β-lactamses have a serine residue for the catalytic activity, while metallo-β-lactamses have catalytic Zn^{2+} ions important for the catalytic activity. The Bush and Jacoby classification scheme of β-lactamases is based on substrate/inhibitor specificity (functional classification, Table 3) [68], and has recently been updated in order to accommodate newly discovered β-lactamses [69].

Table 3: Functional, molecular classification, and properties of β-lactamases (adapted from Bush K et al., 1995 and 2011) [68, 70].

Bush - Jacoby group	Molecular class	Preferred substrates	Inhibition		Representative enzymes
			CA	EDTA	
1	C	Penicillins, Cephamycins, Cephalosporins, Aztreonam	-	-	MIR-1, CMY-2,FOX-1, P99
1e	C	Penicillins, Cephamycins, E-S cephalosporins, Aztreonam	-	-	GC1, CMY-37
2a	A	Penicillins	+	-	PC1 and other staphylococcal penicillinases
2b	A	Penicillins, early cephalosporins	+	-	TEM-1, TEM-2, SHV-1, TLE-1
2be	A	Penicillins, Monobactams, E-S cephalosporins	+	-	TEM-10, TEM-26, SHV-2 to SHV-6, CTX-M-15, CTX-M-44, PER-1, SFO-1, VEB-1, ESBLs
2br	A	Penicillins, early cephalosporins	±	-	TEM-30, TME-76, TEM-103, SHV-10, SHV-26
2ber	A	Penicillins, monobactams, E-S cephalosporins	+	-	TEM-50, TEM-68, TEM-89
2c	A	Carbenicillins	+	-	PSE-1, CARB-3
2d	D	Cloxacillin or Oxacillin	±	-	OXA-1, OXA-10, PSE-2
2de	D	Penicillins, E-S cephalosporins	±	-	OXA-11, OXA-15
2df	D	Carbapenems, Cloxacillin	±		OXA-23, OXA-48
2e	A	Cephalosporins	+	-	CepA
2f	A	Penicillins, Cephamycins, Cephalosporins, Carbapenems	+	-	IMI-1, KPC-2, KPC-3, NMC-A, SME-1, GES-2
3a	B	Penicillins, Cephamycins, Carbapenems, Cephalosporins	-	+	IMPs, VIMs, NDMs, GIM-1, BcII, CcrA, L1, AIM-1, FEZ-1
3b	B	Carbapenems	-	+	CphA, Sfh-1

CA: Clavulanic acid; EDTA: Ethylenediaminetetraacetic acid; E-S: expanded-spectrum; +: positive; -: negative; ±: partially inhibited.

1.5 Metallo-β-lactamases (MBLs):

Metallo-β-lactamases belong to the metallo-hydrolase superfamily [71]. The first MBL enzyme was identified from *Bacillus cereus* (BcII) in 1966 and exhibited interesting properties, including cephalosporinase activity and inhibition by EDTA [61]. Initially MBLs were discovered in environmental and opportunistic Gram-negative bacteria. However, about two decades later, MBLs were discovered in many clinically important pathogenic bacteria [72, 73]. MBL genes are often found in some environmental inhabitant bacteria [72]. The reasons behind maintaining the MBL genes by these environmental inhabitant bacteria is unclear and if they have any normal cellular function [65]. So far, studies have shown that MBL genes are found either intrinsically on chromosomes or acquired by horizontal gene transfer (acquired MBLs) [72].

MBLs have become one of the major factors of resistance towards β-lactams over the past few decades. Further, MBLs exhibits broad-spectrum activity and hydrolyses virtually all classes of β-lactams with the exception of monobactams, e.g. aztreonam [74, 75]. The active site in MBLs contains either 1 or 2 Zn^{2+} ions, coordinated by conserved amino acids and polarized water molecule(s) necessary for the hydrolysis of β-lactams [76]. All the MBLs share a common feature of being inhibited by EDTA and other metal chelating agents, due to the metal dependent catalytic mechanism. The hydrolysis mechanism is unique for MBLs compared to other β-lactamases as no stable or pseudo-stable covalent intermediate is formed during hydrolysis [74]. Hence, they are not inhibited by classical serine β-lactamse inhibitors such as clavulanic acid, tazobactam, and sulbactam [75, 77]. In addition, no clinical inhibitor is currently available to inhibit the activity of MBLs. In general, all MBLs share a common four layer “αβ/βα” motif, with a central “ββ”- sandwich with Zn^{2+} ion(s), and two α-helices on either side [78, 79], which suggests as they all evolved from a common ancestor [80, 81].

1.5.1 Chromosomally encoded MBLs:

The chromosomally encoded MBLs include *B. cereus* (BcII) [82], *Bacteroides fragilis* (CcrA) [83], *Bacillus anthracis* (bla2) [84], *Alcalophilic Bacillus species* (Bce-170) [85], *Chryseobacterium indologenes* (INDs) [86, 87], *Chryseobacterium meningosepticum* (BlaBs) [88-90], *Chryseobacterium gleum* (CGB-1) [90], *Myroides odoratus* (TUS-1) [91], *Myroides odoratimimus* (MUS-1) [91], *Flavobacterium johnsoniae* (JOHN-1) [92], *Aeromonas hydrophila* (CphA) [93], *Aeromonas veronii* (ImiS and AsbM1) [94, 95], *Serratia marcescens* [96], *Elizabethkingia meningoseptica* [88], *Stenotrophomonas maltophilia* (L1) [97], *Legionella gormannii* (FEZ-1) [98], *Caulobacter crescentus* (Mbl1b and CAU-1) [99], *Janthinobacterium lividium* (THIN-B) [100], *C. meningosepticum* (GOB-1) [87], and *Serritia fonticola* (SFH-1) [101]. The first silent gene coding for MBL was discovered in *B. anthracis* [84]. Further, bla_{CifA} shown to be another silent MBL gene found in *B. fragilis* [102]. The chromosomal MBLs generally vary little from one to others [65], irrespective of genus or species.

1.5.2 Acquired MBLs:

The rapid dissemination of acquired MBLs into the clinically important Gram-negative pathogenic bacteria like *P. aeruginosa, A. baumannii* and *Enterobacteriaceae* species such as *K. pneumoniae*, are worrisome [65, 72, 103]. Further, the MBL genes are often carried along with other resistance genes resulting in multi-drug resistance limiting treatment options [65]. The rapid dissemination of MBLs is due to the association of MBL genes with mobile genetic elements such as plasmids, transposons, and IS*CR* elements [65, 72]. So far, the origin of acquired MBLs is still unknown, but it is believed that they originate from environmental bacteria and Gram-negative fermenters [72]. The dissemination of acquired MBLs is a major issue regarding the treatment of individual patients, and confronting infection control polices [72]. Identification of transferable MBLs in various *Enterobacteriaceae* species in Greece stands as an

example of the dissemination rate of MBLs. Moreover, NDMs are being reported from many countries since the first report in 2009 [104, 105].

1.5.3 Global epidemiology of acquired MBLs:

The first acquired MBL gene identified was *bla*$_{IMP}$ reported from Japan in *P. aeruginosa* [106]. Subsequently other acquired MBLs; VIMs, NDMs, SPM-1, GIM-1, SIM-1, DIM-1, TMB-1, KHM-1, AIM-1, and SMB-1 have been identified (Table 4) [65, 72]. On a global scale IMPs, VIMs, NDMs, and to some extent SPM-1 are the most prevalent MBLs. The other MBLs have only been detected in single cases or in a limited geographical region. Among the IMP, VIM, and NDM MBLs several variants have been identified. So far, 36 variants of IMP and 34 variants of VIM have been identified, while for NDM 6 variants have been identified (http://www.lahey.org/Studies). The amino acid similarity between different variants ranges from 87.1% to 99.7% for the IMPs, 74.3% to 99.6% for the VIMs, and 98.6% to 99.6% among NDM variants (Figure 5-7).

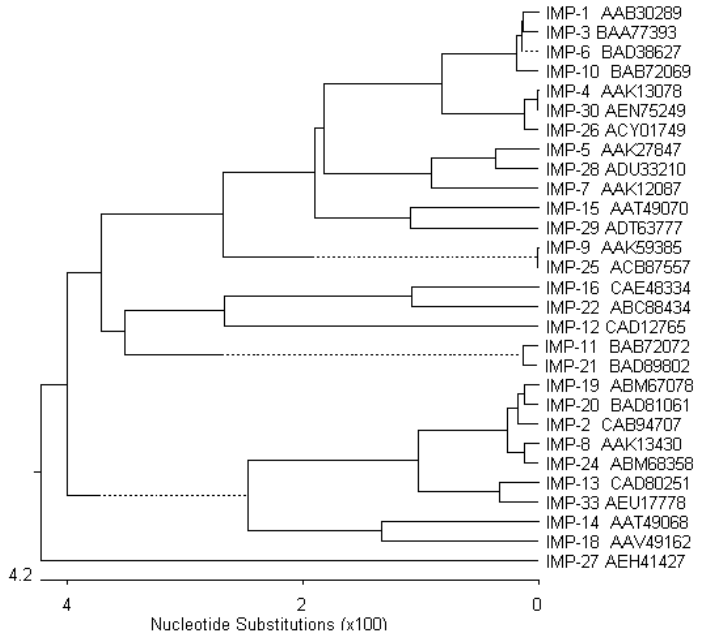

Figure 5: Phylogeny of IMP-type MBLs.

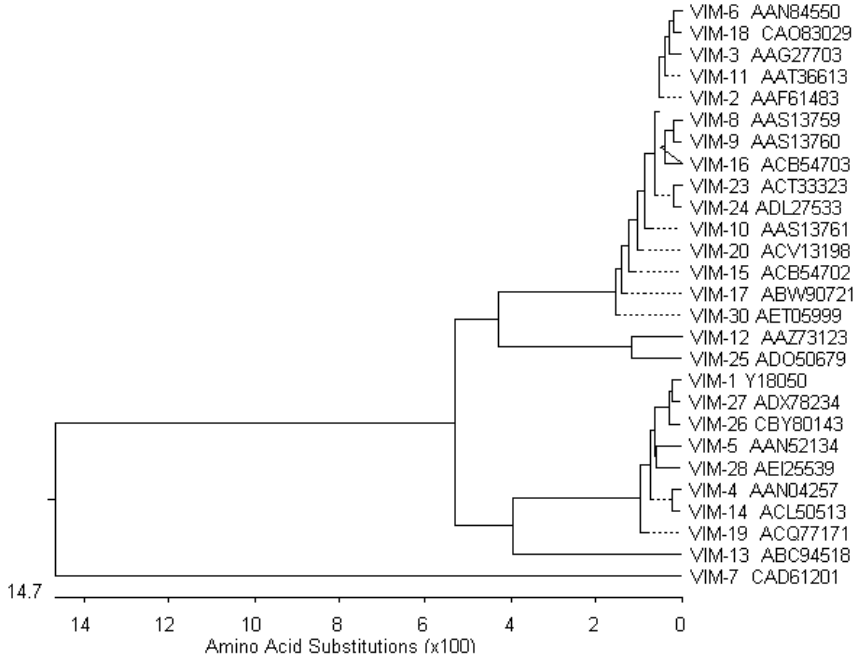

Figure 6: Phylogeny of VIM-type MBLs.

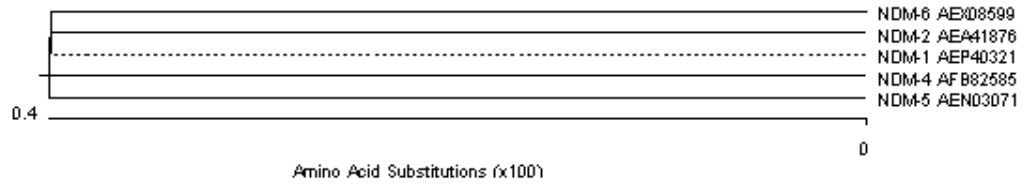

Figure 7: Phylogeny of NDM-type MBLs.

Table 4: Acquired MBLs with bacterial hosts and origins.

MBL-type	Host	Origin	References
IMPs (IMP-1 to IMP-36)	*P. aeruginosa, Pseudomonas putida, Pseudomonas mendocina, Pseudomonas fluorescens, Pseudomonas stutzeri, A. baumannii, Acinetobacter lwoffii, E. coli, S. marcescens, Proteus mirabilis, Alcaligenes xylosoxidans, K. pneumoniae, Klebsiella oxytoca, Shigella flexneri, Aeromonas caviae, Providencia rettgeri, Alcaligenes faecalis, Citrobacter freundii, Enterobacter aerogenes, Enterobacter cloacae, Proteus vulgaris,*	Japan, Korea, Brazil, Singapore, England, Italy, Hong Kong, China, Australia, Portugal, Canada, Malaysia, Taiwan, USA, Norway	[65, 72, 107, 108]
VIMs (VIM-1 to VIM-34)	*P. aeruginosa, P.putida, P. fluorescens, P. stutzeri, A. baumannii, A. hydrophila, S. marcescens, A. xylosoxidans, K. pneumoniae, C. freundii, , E. cloacae, E.coli, Providencia stuartii, Proteus mirabilis, E. aerogenes,*	Italy, Korea, Singapore, Greece, France, Spain, Chile, Croatia, Algeria, Columbia, Venezuela, Argentina, Portugal, Sweden, Poland, USA, Norway, India, Taiwan, Turkey, Mexico, Japan,	[65, 72, 109]
NDMs (NDM-1 to NDM-6)	*K. pneumoniae, A. baumannii, P. stuartii, P. aeruginosa*	India, Sweden, France, Norway, Denmark, UK, Netherlands, Algeria, Afghanistan, China, South Africa, Mauritius, UAE, Egypt, Israel, Korea, Germany, Italy	[105, 110-115]
Others (GIM-1, DIM-1, SPM-1, KHM-1, SIM-1 TMB-1, AIM-1, SMB-1)	*P. aeruginosa, S. marcescens, P. stutzeri*, A. xylosoxidans, *A. baumannii*, *C. freundii*	Germany, Libya, Netherlands, Brazil, Australia, Korea, Japan	[65, 116-118]

1.5.4 Sub-classification of MBLs:

According to the Ambler classification of β-lactamses, MBLs belong to class B [67]. Further, based on the diversity in amino acid sequence and structural properties, MBLs can be subdivided into three subclasses; B1, B2, and B3 [119, 120]. Each subclass contains many different MBLs and variants. Moreover, three dimensional structures of MBLs has shown that these subclasses have substantial differences based on the Zn^{2+} coordinating residues in the active site, number of Zn^{2+} ions at the active site, and loop regions. Further, a standard numbering scheme has been proposed for MBLs (BBL numbering), based on the Zn^{2+} coordinating residues [120] [69]. The BBL numbering scheme is used throughout in this thesis. According to the BBL numbering scheme, a minimum cut-off of 70% amino acid diversity is used to assign new MBLs into the correct subclass [121]. However, the standard numbering scheme was found not to be suitable for all MBLs, as observed for SPM-1 [122]. Based on the functional classification, MBLs are classified into group 3 [68]. Later, this classification has been updated further sub-grouping MBLs according to their hydrolytic properties into group 3a, group 3b, and group 3c [77], as described in Table 3. However, in the latest update, the group 3c was removed [64].

1.5.4.1 B1 MBLs:

Subclass B1 enzymes are monomeric enzymes with two Zn^{2+} ions (bi nuclear) in the active site, with the exception of available mononuclear BcII enzymes. MBLs belonging to the B1 subclass share about 23% identity at the amino acid level [71] (not variants), and contains a large number of different MBLs. These enzymes show broad-spectrum activity towards most β-lactams including carbapenems [71, 75] with the exception of SFB-1 from *Shewanella frigidi* which show reduced activity towards benzylpenicillin, ticarcillin, meropenem, and third generation cephalosporins [123]. Subclass B1 is well characterized with a large number of solved three dimensional structures, compared to the B2 and B3

subclasses. The B1 subclass harbors MBLs which are chromosomal encoded such as BcII from *B. cereus* [82], CcrA from *B. fragilis* [83], BlaB from *C. meningosepticum* [88-90], and acquired MBLs such as IMPs, VIMs, NDMs, GIM-1, DIM-1, TMB-1, KHM-1, SPM-1, and SIM-1 [72]. Most of the known acquired MBLs belong to B1 subclass compared to other subclasses.

1.5.4.2 B2 MBLs:

Subclass B2 MBLs are considered as “true” carbapenemases due to their high specificities for hydrolyzing carbapenems [71]. In contrast, B2 MBLs have weak hydrolytic activity towards penicillins and cephalosporins [75, 124] compared to B1 and B3 subclasses. The subclass B2 MBLs have similarities at the amino acid level [125, 126] with the B1 subclass and it has been suggested that they were descended from a common ancestor [127]. However, B2 subclass is characteristic of harbouring one Zn^{2+} ion in their active site required for β-lactam hydrolysis. Subclass B2 MBLs are less numerous, and have 51% diversity at amino acid level among themselves. As reported so far, all the subclass B2 enzymes are monomeric, and are so far only described as chromosomally encoded [65] such as CphA from *A. hydrophila* [93], ImiS from *Aeromonas veronii* [94], and SFH-1 from *S. fonticola* [101].

1.5.4.3 B3 MBLs:

Subclass B3 enzymes are generally found to be intrinsically located on the chromosome, with the exception of bla_{L1} found to be located on the chromosome or on a plasmid in *S. malthophilia* [128] and, AIM-1 and SMB-1, which have been found to be acquired by *P, aeruginosa* and *S. marcescens*, respectively [118] (Yong, D et al, to be published). Other examples of subclass B3 enzymes includes GOB-1 from *C. meningosepticum* [87], FEZ-1 from *L. gormannii* [98], THIN-B from *J. lividium* [100], Mbl1b [99] and CAU-1 [129] from *Caulobacter*

crescentus, BJP-1 from *B. Japonicum* [130]. Most of the B3 MBL producing bacteria are environmental inhabitants and non-pathogenic. B3 enzymes harbour two Zn^{2+} ions at their active site. With the exception of L1 (tetramer), all are monomeric enzymes in this subclass. The structure of L1 revealed that the hydrophobic pocket formed by Met175 with Leu1544, Pro198, and the long N-terminal tail are responsible for inter-monomeric interactions, leading to tetramerization of L1 [97].

1.5.5 Three dimensional structures of MBLs:

1.5.5.1 Overall structure:

The mono-zinc form of BcII was the first solved MBL structure [131], and revealed the αβ/βα protein fold of MBLs. Since, then many structures of MBLs from all three subclasses have been solved providing insightful information of these enzymes (Table 5).

Table 5: Available three dimensional structures of subclass B1, B2, and B3 MBLs with their PDB code (http://www.rcsb.org/pdb/home/home.do).

Subclass	Enzymes	PDB code	References
B1 subclass	BcII	1BMC, 1BVT, 1BC2, 2BC2, 3BC2, 1DXK, 2NZE, 2NYP, 2NXA, 3I11-3I15, 3KNS, 3I0V	[78, 131, 132]
	CcrA	1ZNB, 2ZNB, 3ZNB, 4ZNB, 2BMI, 1A7T, 1A8T, 1HLK, 1KR3,	[133-135]
	SPM-1	2FHX	[136]
	IMP-1	1DDK, 1JJE, 1JJT, 1DD6, 2DOO	[79, 137, 138]
	VIM-2	1KO2, 1KO3, 2YZ3	[139, 140]
	VIM-4	2WRS	[141]
	IND-7	3L6N	[142]
	NDM-1	3Q6X, 3RKJ, 3RKK, 3SBL, 3SFP, 3ZR9, 3SRX, 3SPU, 3PG4	[143-146]
B2 subclass	CphA	1X8I, 1X8H, 1X8G, 2GKL, 2QDS	[147]
	SFH-1	3Q6V	[148]
B3 subclass	L1	1SML, 2AIO, 2FM6, 2FU6-2FU9, 2GFJ, 2GFK, 2H6A, 2HB9, 2QIN, 2QJS, 2QDT	[97, 149-152]
	FEZ-1	1JT1, 1KO7, 1L9Y	[153]
	BJP-1	3M8T, 3LVZ, 2GMN, 1ERO	[154]

All MBLs share a common characteristic fold (αβ/βα) and catalytic mechanism or function, which suggests that they all evolved, from common ancestor [80, 81]. In addition, they share less than 25% sequence similarities at amino acid level (not between variants) [65], which represents the diversity of MBLs. Further, the three dimensional structures of all MBLs indicates that they have arisen from gene duplication (two halves of the “αβ” fold) [131]. The overall structure for all MBLs contains two β-sheets at the core and five α-helices external to them with variable loops which connects the α-helices and β-sheets (Figure 8). The active site groove is located in the interface formed by the core β-sheets (ββ) for the best possible interactions with the substrates [155]. Despite a common fold and conserved motifs in the three dimensional structure, notable differences for each subclass like active site Zn^{2+} ion(s) coordinating residues, number of Zn^{2+} ions at active site, and loop regions are observed [69, 156]. Further, intramolecular disulphide bridges were observed as a unique property of B3 subclass MBLs and suggested to play an important role in protein folding. In L1, and FEZ-1 structures, an intramolecular bridge was observed between the residues Cys256-Cys290 and between residues Cys200-Cys220 in BJP-1 [97, 153, 154].

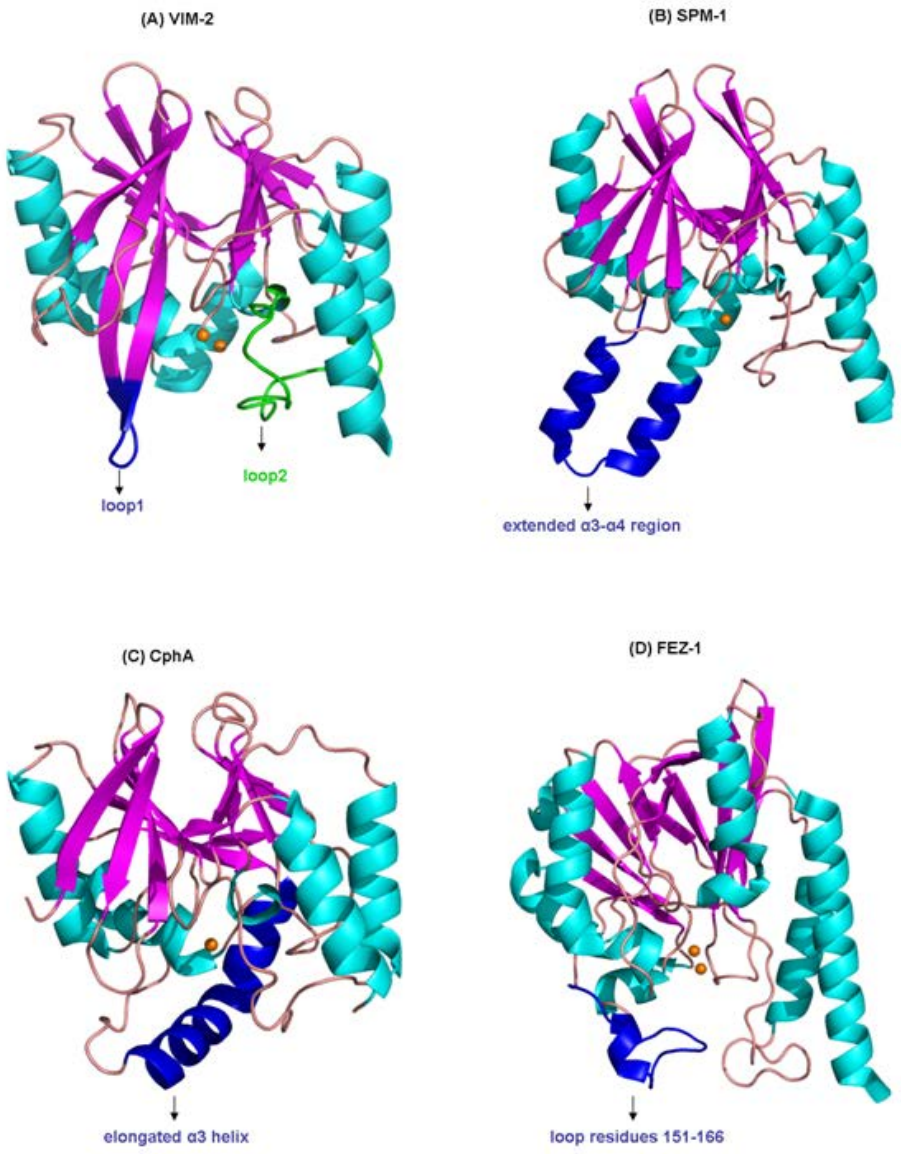

Figure 8: Three dimensional structures of MBLs; (A) VIM-2 (PDB id: 1KO3, B1 subclass), (B) SPM-1 (PDB id: 2FHX, B1 subclass), (C) CphA (PDB id: 1X8G, B2 subclass) and (D) FEZ-1 (PDB id: 1K07, B3 subclass). Zn^{2+} *ion(s) represented as spheres in orange colour and loop regions in blue colour (loop 2 region in green colour for VIM-7). All figures were generated by PyMol.*

With respect to the various loops, the B1 subclass with the exception of SPM-1 contains an important flexible or flapping loop referred to as loop 1 formed by residues 60-66 from the N-terminal domain [71, 157]. This loop1 is shown to be interacting with bound substrates (or) inhibitors [71, 79, 158, 159]. Based on the available B1 MBLs structures, both native and in complex with inhibitors structures suggest that, loop 1 is flexible in the native enzymes [158]. However, loop 1 can be stabilized or immobilized when an inhibitor is bound to the enzyme [79, 160]. Thus, loop 1 entrap the substrate at the active site [158, 161, 162], hence, deletion of loop 1 show notable decrease in the enzyme activity [158, 163]. Furthermore, the loop 2 region composed of residues 223-242 [164, 165] has also been suggested to influence the substrate or inhibitor interactions. The SPM-1 structure is some extent different compared to other B1 subclass by lack of loop 1 and a short β3-β4 of five residues, however, it harbours a central insertion of a 24 amino acid long α3-α4 region (residues 150b-165) [157]. Deletion of this elongated loop has shown marginal effect on the enzyme affinity, and activity towards substrates [157]. The structural features and sequence identities of SPM-1 are between the B1 and B2 subclass suggesting that it is a structural hybrid to B1 and B2 subclasses [71].

In subclass B2 and B3 MBLs, the loop 1 region is absent [71]. In contrast, B2 subclass harbours an elongated α3 helix (residues 140-161), close to the active site. In CphA, it was suggested that this loop is structured as a curvature on the surface of the enzyme, and thus enhances the possibilities for substrates to bind, particularly carbapenems [147]. The B3 subclass is characterized by a loop 2 formed by the residues between helix α3 and β-strand β7 (residues from 156-166). This loop region in B3 subclass is located near to the active site [153]. Further, mutational studies involving loop 2 residues in B3 subclass MBL, L1 suggests that substrates will interact with loop 2, and exhibited variations in the affinity and catalytic efficiency [166].

1.5.5.2 Active site and Zn-binding residues:

The active site of MBLs is well defined and harbours special residues which interact with the catalytic Zn^{2+} ion(s). However, the Zn^{2+} ion(s) coordinating residues and number of Zn^{2+} ions at the active site varies among the B1, B2, and B3 subclasses, (Figure 9). The active site of subclass B1 and B3 posses two catalytic Zn^{2+} ions (with the exception of mono-zinc B1 MBLs), in contrast subclass B2 MBLs are active as mono-zinc enzymes.

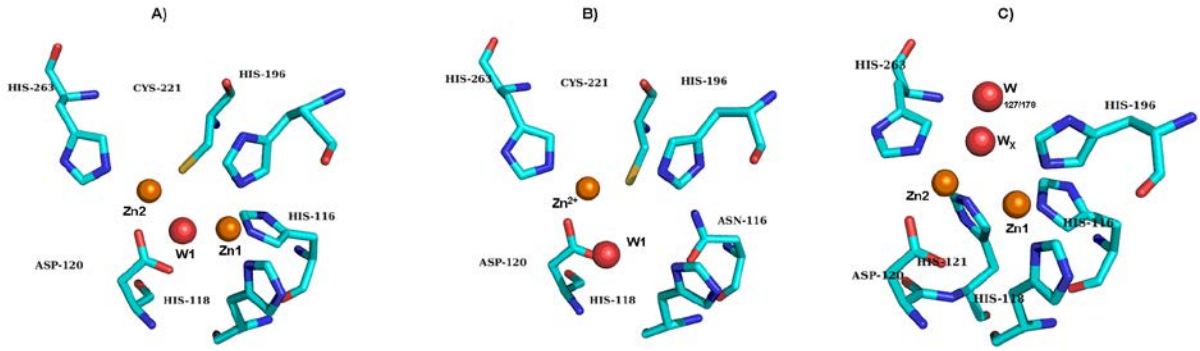

Figure 9: Zinc sites and metal ligands architecture at active site; (A) VIM-2 (PDB id: 1KO3, B1 subclass), (B) CphA (PDB no: 1X8G, B2 subclass) and (C) FEZ-1 (PDB no: 1K07, B3 subclass). All figures were generated by PyMol (modified from Bebrone C, 2007) [71].

The overall structure of B1 subclass is well organized and can be made into two halves which are connected by catalytic Zn+ ions [167]. In the active site, one Zn^{2+} ion (Zn1) is coordinated by the residues His116-His118-His196 (“histidine site”) and a water molecule by a tetrahedral coordination. The other Zn^{2+} ion (Zn2) is coordinated by residues Asp120-Cys221-His263 (“cysteine site”) and two water molecules by trigonal bipyramidal coordination. The same water molecule (usually W1 or Wx) is shared by or link both Zn^{2+} ions and acts as a nucleophile during hydrolysis [133, 168]. As mentioned subclass B1 possesses two potential Zn^{2+} ions at the active site, with the exception of the initially solved mono-zinc form of BcII (PDB id: 1BMC) [131]. However, other solved structures of BcII (PDB

ids: 1BC2, 1BVT) and spectroscopic studies have shown two Zn^{2+} ions in the active site [134, 165, 169]. In addition, the mono-zinc form of BcII, VIM-2 (PDB id: 1KO3), and SPM-1 structures suggests that the Zn^{2+} ion is present at the "histidine site" [131, 139, 157]. Further, the catalytic Zn^{2+} ions affinities are different among B1 subclass MBLs, such as IMP-1 and CcrA contains two high affinity zinc sites, whereas BcII exhibit affinity variations between Zn1 and Zn2 sites [71].

Subclass B2 is different from B1 and B3 subclasses with a single Zn^{2+} ion at the active site. The active site of CphA structure suggests that the catalytic Zn^{2+} ion is present in the "cysteine site" [147]. The Zn2 site is still to be elucidated. Further, in the B2 subclass His116 is replaced by Asn116 in the "histidine site" and thus provides an environment for the coordination of mono-zinc ion with Asp120, Cys221, and His263 residues [147].

Like the B1 subclass, subclass B3 MBLs possesses two catalytic Zn^{2+} ions at the active site with the exception of the debatable mono-zinc GOB-I [71, 125]. However, the Zn^{2+} ions coordinating residues or sites are different compared to B1 subclass. In the B3 subclass, the "histidine site" is the same as in the B1 subclass but divergent for the Zn2 site which harbours His121 replacing the Cys221 compared to B1 and B2 subclasses as a metal ligand. The second Zn^{2+} ion is coordinated by Asp120-His121-His263 and two water molecules by trigonal bipyramidal coordination [97, 153]. However, a remarkable exception of B3 subclass is found for GOB enzymes where metal ligands His116 and Ser221 are replaced by Gln116 and Met221, respectively [170]. The same water/OH^- molecule shared by both Zn1 and Zn2 sites, acts as nucleophile similar to the B1 subclass [97].

The subclass B1 enzymes are active in mono and di-zinc forms, but it is suggested that binding of the second Zn^{2+} ion enhances the activity as observed for BcII [171]. In contrast, B2 subclass enzymes such as CphA and ImiS are

active in mono-zinc form only, and the binding of second Zn^{2+} ion reduced the catalytic efficiency of CphA [172]. The subclass B3 enzymes are active in di-zinc form only as observed for L1 [75]. It has been suggested that Arg121 might be responsible for the variations in Zn^{2+} ion affinities. The residue Arg121 (positively charged amino acid) is conserved in subclass B1 and B2, with the exception of CcrA and IMP-1 in which Arg121 is replaced by Ser121 and Cys121 (neutral amino acids), respectively. Thus, CcrA and IMP-1 exhibit enhanced affinity for both zinc sites compared to others. In contrast, His121 is present at this position in B3 subclass, thus exhibit enhanced affinities towards both Zn^{2+} ions [71].

1.5.6 Biochemistry of MBLs:

MBLs harbour a wide plastic and well defined active site, and hydrolyze most of the β-lactams efficiently, with the exception of aztreonam [75]. All the MBLs share common features regarding their activity like; a) good to excellent carbapenemase activity; b) inhibition by EDTA or other metal chelators; and c) lack of activity on monobactams [173]. In general, subclass B1 MBLs show a broad-substrate profile which includes penicillins, carbapenems (efficient hydrolysis), and cephalosporins (overall lower hydrolysis compared to penicillins and carbapenems) [174]. In contrast, subclass B2 MBLs hydrolyzes carbapenems efficiently but show weak catalytic efficiencies towards penicillins and cephalosporins, while subclass B3 enzymes, hydrolyses cephalosporins efficiently compared to penicillins and carbapenems [174].

The affinity of an enzyme to substrate is referred to as the K_m, the enzyme's ability to turn over the substrate is referred as the k_{cat}, and the overall enzyme's catalytic efficiency can be measured as the k_{cat}/K_m. These kinetic parameters are influenced by the substrates for hydrolysis, the active site architecture, Zn^{2+} ion(s), and residues close to the active site.

Overall the affinity (K_m), turnover (k_{cat}), and the overall catalytic efficiency (k_{cat}/K_m) for different substrates varies not only between different MBLs/subclasses but also between variants (Table 6 and 7) [175].

Table 6: Steady state kinetics of B1 subclass MBLs GIM-1, IMP-1, VIM-7 and VIM-2 [176, 177].

Substrate	**GIM-1**			**IMP-1**			**VIM-7**			**VIM-2**		
	k_{cat} (s^{-1})	K_m (μM)	k_{cat} / K_m ($\mu M^{-1}.s^{-1}$)	k_{cat} (s^{-1})	K_m (μM)	k_{cat} / K_m ($\mu M^{-1}.s^{-1}$)	k_{cat} (s^{-1})	K_m (μM)	k_{cat} / K_m ($\mu M^{-1}.s^{-1}$)	k_{cat} (s^{-1})	K_m (μM)	k_{cat} / K_m ($\mu M^{-1}.s^{-1}$)
Ampicillin	3.3	20	0.16	950	200	4.8	190	15	1.3	125	90	1.4
Piperacillin	6.9	69	0.10	ND	ND	ND	140	26	5.4	300	125	2.4
Nitrocefin	5.8	12	0.47	63	27	2.3	1500	58	26	770	18	42.8
Cephalothin	1.6	22	0.72	48	21	2.4	180	45	4	130	11	12
Cefuroxime	5.9	7	0.80	8	37	0.22	16	29	0.55	8	20	0.4
Cefoxitin	8.3	206	0.04	16	8*	2	10	68	0.15	15	13	1.2
Ceftazidime	18	31	0.58	8	44	0.18	1.4	120	0.012	3.6	72	0.05
Cefotaxime	1.1	4	0.24	1.3	4*	0.35	56	22	2.6	70	12	5.8
Cefepime	17	431	0.04	7	11*	0.66	5.3	580	0.0091	40	400	0.1
Imipenem	27	287	0.09	46	39	1.2	100	27	3.7	34	9	3.8
Meropenem	2.7	25	0.11	50	10	0.12	42	38	1.1	5	2	2.5
Moxalactam	14	1,035	0.01	88	10*	8.8	ND	ND	ND	90	55	1.6

"ND": no data available; and *, k_m was obtained as the K_i value.

Table 7: Steady state kinetics of B3 subclass MBLs AIM-1, BJP-1 [130, 154], FEZ-1 [178], and L1 [179].

Substrate	**AIM-1**			**BJP-1**			**FEZ-1**			**L1**		
	K_m (μM)	k_{cat} (s^{-1})	k_{cat}/K_m (s^{-1}/M)	K_m (μM)	k_{cat} (s^{-1})	k_{cat}/K_m (s^{-1}/M)	K_m (μM)	k_{cat} (s^{-1})	k_{cat}/K_m (s^{-1}/M)	K_m (μM)	k_{cat} (s^{-1})	k_{cat}/K_m (s^{-1}/M)
Penicillin G	110 ± 21	590± 31	$5.4x10^6$	130	18	1.3 x 10^5	590	70	1.1 x 10^5	50	1110	2.2 x 10^7
Ampicillin	24 ± 3	150± 5	$6.3x10^6$	670	13	1.3 x 10^4	>5000	>5.5	1.1 x 10^4	40	175	4.4 x 10^6
Cefoxitin	22 ± 2	52 ± 1	$2.4x10^5$	140	10	7.1 x 10^4	11	3	2.7 x 10^5	2	1.1	5.5 x 10^5
Cefuroxime	35 ± 4	170 ± 5	$4.8x10^6$	115	58	5.0 x 10^5	50	320	6.4 x 10^5	30	80	2.7 x 10^6
Ceftazidime	730 ± 180	46 ± 7	$6.3x10^4$	>700	>3	4.3 x 10^3	>1000	>4	4.0 x 10^3	145	27	0.2 x 10^6
Cefepime	440 ± 60	37 ± 1	$8.4x10^3$	>400	>0.08	2.0 x 10^2	>1000	>6	6.0 x 10^3	130	0.33	2.5 x 10^4
Imipenem	410 ± 16	2200 ± 50	$5.4x10^6$	260	15	6.0 x 10^4	>1000	>200	2.0 x 10^5	90	65	7.3 x 10^5
Meropenem	41 ± 4	760 ± 16	$1.8x10^7$	190	156	8.3 x 10^5	85	45	5.0 x 10^5	13	77	5.9 x 10^6
Ertapenem	45 ± 4	340 ± 9	$7.5x10^6$	ND	ND	ND	ND	ND	ND	ND	ND	ND

"ND": no data available.

The affinity (K_m) towards substrates also varies between MBLs. For instance, SPM-1 and L1 exhibit higher affinities towards most of the substrates, whereas IMP-1 and FEZ-1 exhibit higher affinities towards cephalosporins and meropenem compared to other MBLs. Similarly, the turnover rate of MBLs varies between MBLs, for example BcII and FEZ-1 hydrolyses with high turnover rates and lower affinities, whereas VIM-2 hydrolyses with high affinities and lower turnover rates towards carbapenems. In general, some MBLs such as IMP-1,

VIM-2, and SPM-1 exhibit higher overall catalytic efficiency towards most of the substrates compared to others such as BcII, FEZ-1, and GIM-1

The differences in kinetic parameters between two enzymes can best be compared when both enzymes kinetics data were collected under the same experimental conditions [175]. Thus, the kinetic data can lead to analysis of the functional differences in respect to the structural differences [175]. For instance, VIM-1 and VIM-2 are the two variants from VIM-family, and are 93% similar at the amino acid level. The VIM-2 enzyme kinetics data for different substrates (penicillins, cephalosporins, and carbapenems) was collected under the same conditions used for VIM-1 kinetics data [175, 180].

The VIM-2 hydrolyses penicillins efficiently with the exception of temocillin compared to VIM-1 (50-100 folds), due to lower turnover rate (k_{cat} value) [175]. Further, VIM-2 hydrolyses quite efficiently benzylpenicillin and ampicillin compared to VIM-1. Whereas VIM-1 hydrolyse azocillin efficiently with high turnover rate compared to VIM-2. The carbencillin and mezocillin kinetics parameters were nearly similar for both VIM-2 and VIM-1. In addition, the piperacillin, ticarcillin and temocillin hydrolytic efficiencies were comparable between VIM-1 and VIM-2. However, the affinity (K_m value) variations of ticarcillin and temocillin were significant between VIM-1 and VIM-2. It was suggested that the presence of the 6-α-methoxy group in temocillin was responsible for the affinity variations between VIM-1 (decreased K_m value) and VIM-2 (increased K_m value) in respect to the structural differences. Towards cephalosporins, VIM-2 exhibit lower k_{cat} and K_m values compared to VIM-1 with the exception of cefepime (40-fold higher). The overall hydrolytic efficiencies of VIM-1 and VIM-2 (k_{cat}/K_m) were different for substrates such as cefoxitin, cefuroxime, cefotaxime, and moxalactam, whereas comparable towards cefaloridine, cefalothin, ceftazidime and cefpirome. Further, VIM-2 exhibit higher affinity (K_m value) towards ceftazidime, compared to VIM-1. The hydrolytic efficiencies towards carbapenems by VIM-1 and VIM-2 were notable different. The imipenem and

meropenem were quite efficiently hydrolysed by VIM-2 (30 and 10 folds, respectively) compared to VIM-1 due to higher turnover rate and lower K_m values. The docking experiments with benzylpenicillin into the VIM-1 and VIM-2 active site revealed that the amino acid substitutions at positions 224 and 228 between these enzymes are responsible for the variations of kinetic parameters. It was suggested that VIM-1 has a shorter and mostly neutral His224 residue, whereas VIM-2 has longer and positively charged Tyr224 residue. Thus, the Tyr224 of VIM-2 might affect the stabilization of the positively charged C3 group of ceftazidime compared to His224 of VIM-1. Further, the long, positively charged Arg228 in VIM-2 which protrudes into the active site, might influence the affinity of substrates compared to a short Ser228 residue in VIM-1. The docking data supported that the VIM-2 Arg228 guanidium group interact with the benzylpenicillin carboxylate, whereas VIM-1 Ser228 fail to perform such interactions [175]. Thus, suggested that the kinetic variations between enzymes are due to residue substitutions, and also dependent of the type of substrate.

Further, many studies have investigated the factors involved in the observed variability of kinetic parameters. The Zn^{2+} ions coordinating residues play an important role in the catalytic efficiencies of the MBLs. For instance, in CphA (B2 subclass) the Zn^{2+} ion is coordinated by Asn116 and Cys221 [147], and mutational studies on the CphA enzyme suggested that Cys221Ser or Cys221Ala substitutions seriously impaired the coordination of Zn^{2+} ion resulting in an inactive enzyme, whereas Asn116Cys or Asn116His substitutions enhanced the catalytic efficiencies towards penicillins and cephalosporins, compared to the wild type [181]. The loops close to the active site and the residues from loop regions have also been suggested to influence the kinetic parameters of MBLs. In the B1 subclass, loop 1 and loop 2 residues have been suggested to play an important role, and can influence the kinetic parameters of MBLs towards different substrates, apart from active site residues, and Zn^{2+} ion(s) at the active site. In B3 subclass loop regions formed with residues 156-162 and 223-230 were suggested to perform similar function to cover the active site and interacts with

the substrates, whereas for B2 subclass the loop formed by elongated α3 helix formed with residues 140-161 was suggested [71, 147].

For instance, the steady-state kinetic parameters of the B1 subgroup MBL, VIM-7 in comparison with VIM-1 and VIM-2 against different classes of β-lactams suggest three different trends regarding the overall catalytic efficiency; penicillins: VIM-7>VIM-2>VIM-1, cephalosporins: VIM-1≈VIM-2>VIM-7, and carbapenems: VIM-7≈VIM-2>VIM-1. The VIM-2 structure in comparison with a homology model of VIM-7 and amino acid sequences of other VIMs suggested that residue alterations near the active site, such as Pro68Ser, Tyr218Phe, and Tyr224His for VIM-7 might have an impact regarding the variations towards the overall catalytic differences. These residue alterations which are suggested to define the active site groove and interactions with substrates, hence contribute to variations in the overall catalytic efficiencies of VIM-7 compared to VIM-2 and VIM-1.

1.5.7 Catalytic mechanism of MBLs:

In general, β-lactam hydrolysis by MBLs is carried out first by a nucleophilic attack on the carbonyl group and cleavage of the C-N bond of the lactam ring, followed by triggered protonation of the bridging nitrogen. These steps will be carried out on the same face of the antibiotic [156, 182]. The hydrolysis is unique for MBLs compared to other β-lactamases as no stable or pseudo-stable covalent intermediate is formed during hydrolysis [74, 156], where the Zn^{2+} ion(s), Zn^{2+} ion coordinating residues, and a water molecule carry out an important role in the catalytic activity of MBLs, followed by loops and other conserved residues [65].

It has been demonstrated that during the hydrolysis, the β-lactam carbonyl group might be directly coordinated with the catalytic Zn^{2+} ion(s) [183] or substrate interaction carried out with Zn^{2+} ion(s) by an activated hydroxide ion [167, 184]. The first available BcII structures were mono-zinc forms, and suggested that the hydrolysis is carried out by mononuclear enzymes [131]. However, later

investigation of the BcII enzyme suggested that only the di-zinc form is active for the maximum catalytic activity [185]. Another approach of investigating the Zn^{2+} ion catalytic activity for the BcII enzyme showed that it is active in both mono and di-zinc form suggesting that there are two possible mechanisms in two possible states [186]. However, the number of Zn^{2+} ions required for hydrolysis is still a debatable issue, but it has been suggested that the Zn1 bound water molecule or hydroxide acts as the nucleophile for the hydrolysis in both mono- and di-zinc MBLs of the B1 and B3 subclass [156]. In addition, it has been suggested that the hydrolysis mechanism of MBLs varies based on the substrates [70]. Based on the available three dimensional structures, it has been suggested that the catalytic mechanism of MBLs can be divided into mono and di-zinc mechanisms [156]. The B1 and B3 subclasses perform the di-zinc mechanism in contradiction to 1 or 2 Zn^{2+} ions for BcII enzyme, while for enzymes of the B2 subclass, mononuclear Zn^{2+} carries out the catalytic mechanism.

For the mono-zinc form of the B1 subclass BcII enzyme the catalytic activity has been well investigated and a mechanism has been proposed (Figure 10) [182].

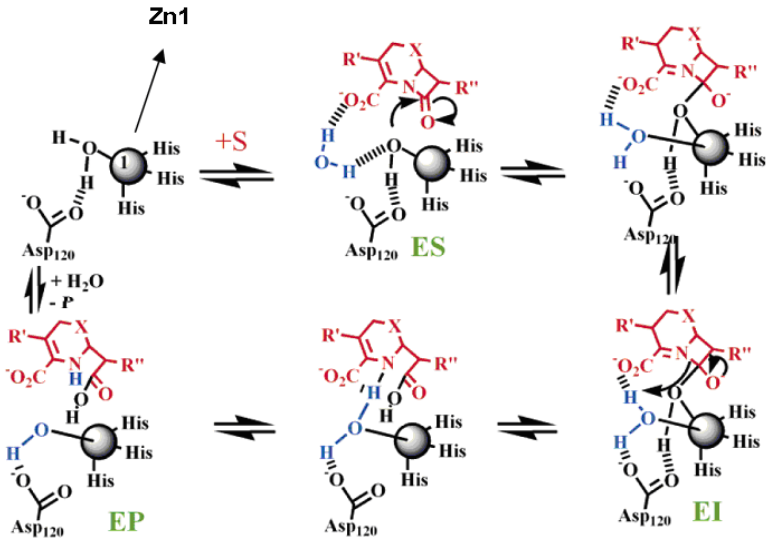

Figure 10: Suggested catalytic mechanism of cephalosporins by mono-zinc B1 subclass [156]. ES: enzyme-substrate; EI: enzyme-intermediate and EP: enzyme-product.

In BcII, the catalytic Zn1 site holds tetrahedral coordination with His116-His118-His196 and a water molecule. This Zn1 ion acts as a Lewis acid and decreases the pK_a value of a water molecule which results into a hydroxide ion at neutral pH. This hydroxide ion carries out the nucleophilic attack on the carboxyl group carbon of the β-lactam and thus aid the formation of a principal tetrahedral intermediate, which will be stabilized by the Zn1 ion. As the same water molecule coordinates both metal sites, Asp120 acts as a general base for the second step of hydrolysis. Further, Asp120 deprotonates the hydroxide ion to generate a dianionic tetrahedral second intermediate stabilized by the Zn1 ion. Further, Asp120 donates a proton to the nitrogen of β-lactam ring and thus assists the ring opening [182]. However, a mutational study on the Asp120 residue has shown in contradiction that it does not act as a proton donor nor has a role in nucleophilic attack [187].

In the mono-zinc B2 subclass, a different catalytic mechanism has been proposed for the enzymes CphA [147] and ImiS (Figure 11) [188].

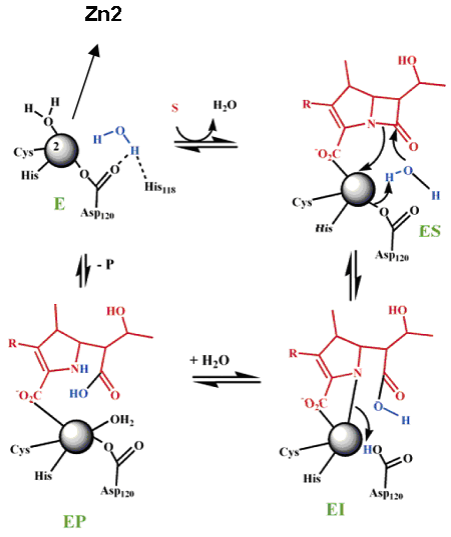

Figure 11: Suggested catalytic mechanism of carbapenems by mono-zinc B2 subclass [156]. E: enzyme; ES: enzyme-substrate; EI: enzyme-intermediate and EP: enzyme-product.

The CphA enzyme complexed with hydrolyzed biapenem suggests that the water molecule perform the nucleophilic attack which is activated by His118 and/or Asp120, but not by the metal coordinated water molecule or hydroxide ion [147, 156, 189]. However, the Zn2 ion might support the C-N bond cleavage by bridging nitrogen coordination [189].

In di-zinc enzymes of B1 and B3 subclasses, CcrA, IMP-1, and L1 are the best studied enzymes using nitrocefin as a substrate (a chromogenic cephalosporin). Based on these studies, a mechanism has been proposed (Figure 12) which suggest that, Zn2 stabilizes the negative charge generated at the nitrogen atom after the C-N bond cleavage, and the protonation is the rate limiting step [168, 185, 190].

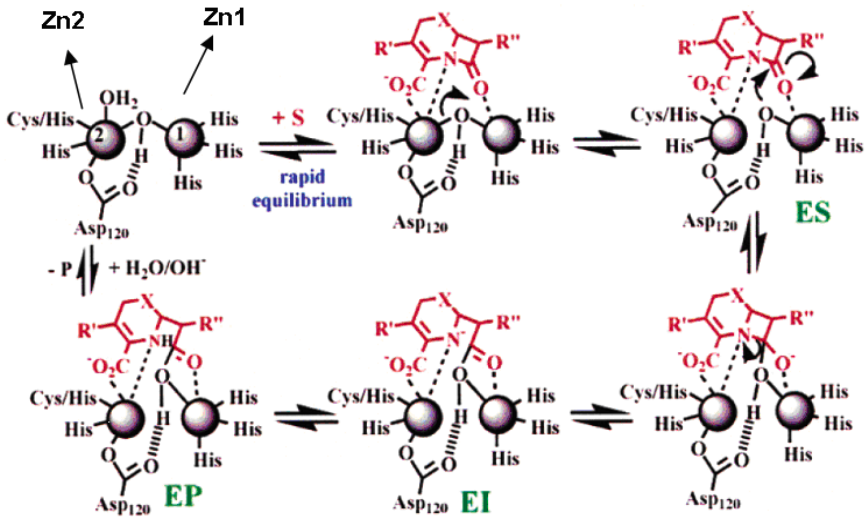

Figure 12: Suggested catalytic mechanism of cephalosporins by di-zinc B1 subclass [156].

Further, with nitrocefin as a substrate, the developed negative charge will be stabilized differently compared to other β-lactams. Whereas towards other β-lactams, hydrolysis is as a rate limiting step, carried out by the cleavage of

tetrahedral intermediate, and occurs simultaneously to the nitrogen protonation of β-lactam ring [191].

1.5.8 MBL inhibitors:

MBLs are not inhibited by classical serine β-lactamase inhibitors such as clavulanic acid, tazobactam, and sulbactam [192, 193]. So far reported inhibitors for MBLs (Table 8), show inhibition towards certain β-lactamses, but not approved for clinical use due to their toxicity. Initial studies for inhibitor investigation have been focused on non-clinical relevant MBLs. However, crystal structures of VIM-2, IMP-1, and FEZ-1 in complex with mercaptocarboxylate inhibitor have provided some information on how inhibitors bind to MBLs [79, 140, 153]. Further, BlaB in complex with D-captopril suggested interactions of inhibitor with MBLs [160]. However, the diversity of MBLs, and active site fold similarities with mammalian enzyme (ex; human glyoxalase-II, Figure 13) [80] are the main obstacles for the development of a successful inhibitor. Hence, no clinically inhibitor is available so far for MBLs. In addition, due to internal diversity with in MBLs, a single inhibitor might not sufficient to be active against all MBLs [80].

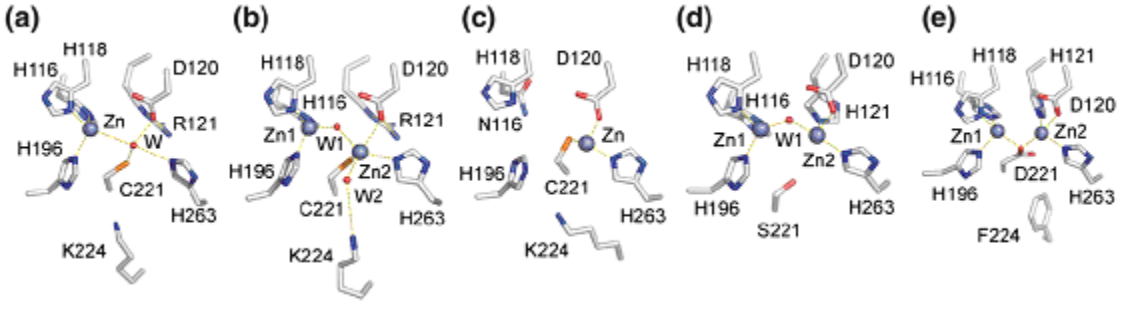

Figure 13: Comparison of MBLs and human glyoxalase-II active site and metal ligands; (a) mono-zinc BcII (B1 subclass), (b) di-zinc BcII (B1 subclass), (c) CphA (B2 subclass), (d) L1 (B3 subclass) and (e) human glyoxalase-II [194].

Table 8: Inhibitors of MBLs. (Modified from Walsh. T.R, et al., 2005) [65].

Type of Inhibitor	Compound	Enzyme tested	References
Thiol	Mercaptoacetic acid	IMP-1	[65]
	Mercaptopropionic acid	IMP-1	
	2'-Mercaptoethyl derivative	BcII	
	Thiobenzoate derivative	IMP-1, CcrA	
	2-*para*-Thiomandelic acid	BcII	
	Quinoline C45H	IMP-1, VIM-2	
Thioester	Morpholinoethanesulfonic acid	CcrA	
	SB217782/8018/9158, SB214752	L1	
	Biphenylmethyl derivatives	IMP-1, CcrA	
Tricyclic products	SB238569	BcII, IMP-1, CcrA	
	2S-3S disubstitute	IMP-1	
1-β-Methyl carbapenem	J-110, 441	IMP-1, CcrA, L1, BcII	
	J-111, 225	IMP-1	
Penicillin derivatives	Penicillinate sulfone Penamaldic derivatives	L1, BcII BcII	
***N*-Arylsulfonyl hydrazone**	2-Napthyl derivatives	IMP-1	
Biphenyl tetrazole	L161, 189	CcrA	
Cysteinyl peptide	D-Phenylalanine derivative	BcII	
Trifluoromethyl Alcohol and ketones	D-Alanine derivative	BcII, L1,	
Thioxocephalosporin	Thioacid	BcII	
Pthalic acid	Pthalic acid derivatives (12f)	IMP-1	[195]
Maleic acid derivatives	ME1071	IMP-1	[196]
Benzohydroxamic acid	2,5-substituted benzophenone hydroxamic acid	FEZ-1	[197]
Mercaptophosphate derivatives	Compound 10a, 18	VIM-4, CphA, FEZ-1	[198]
Triazoles	3-Mercapto-1, 2, 4-triazoles and N-acylated thiosemicarbazides	IMP-1	[199]
Peptides	Peptide derivatives	L1, FEZ-1	[200-202]

2. Aim of the study

The overall aim of this thesis was to study the structural and biochemical aspects of different MBLs to increase the knowledge on this group of β-lactamases.

The main aims of the thesis were:

Paper I: To determine the three-dimensional structure of VIM-7 and binding interactions of β-lactams to VIM-7 and VIM-2 to better understand the relationship between sequence, structure, and activity in VIM MBLs.

Paper II: To determine the kinetic properties of the novel MBL, TMB-1, identified in an *Achromobacter xylosoxidans* strain isolated in Tripoli, Libya.

Paper III: To determine the three-dimensional structure and binding interactions to β-lactams of AIM-1, followed by investigation into the role of Gln157 on the biochemical activity.

Paper IV: To determine the three-dimensional structure of GIM-1 to investigate the structural properties influence on the kinetic activity of the enzyme.

3. Summary of results

Paper I: *"Structural and computational investigations of VIM-7: insights into the substrate specificity of VIM metallo-β-lactamases"*

We solved the three dimensional structure of the native VIM-7 (1.86 Å), VIM-7-Ox (1.70 Å) with Cys221 oxidized, and VIM-7-S (2.33 Å) with a sulphur atom bridging the two active-site zinc ions. The overall structure of VIM-7 showed the characteristic αβ/βα-fold of MBLs. The coordination of the Zn ions in the three structures was different with Zn1 tetrahedrally coordinated in VIM-7 and VIM-7-S,

and pentacoordinated in distorted trigonal bipyramidal geometry in VIM-7-Ox. The Zn2 ion was tetragonally coordinated in the VIM-7-Ox structure a mixture of dizinc (Cys221 bound to Zn2) and monozinc (oxidized cysteine and an empty Zn2 site) was observed. Comparison of VIM-7 with VIM-2 and VIM-4 showed that the structures are closely related with an overall RMSD of C^{α} atoms of 0.49-0.64 Å and that structural differences are confined to residues Pro38-Gly40 (VIM-4) and Lys60-Thr64, Asp76-Ala77, and Gly232-Asn233 (both structures). The structural comparison and the docking studies indicate several amino acid substitutions, particularly residues in loop 1 (residues 60-66) and residues 68, 218, and 224, that could influence the catalytic parameters. In VIM-7, loop 1 is positioned farther away from the active site than in VIM-2 and VIM-4 resulting in a more open active site in VIM-7. In addition residue substitutions results in a less negatively charged surface compared to VIM-2 and an increased flexibility of loop 1. Further, the presence of Phe218 and His224 in VIM-7 disrupts hydrogen-bonding networks close to the active site. The docking data of ceftazidime and cefoxitin into VIM-7 and VIM-2 suggest that residue differences/substitutions may alter the flexibility and conformation of regions such as loop 1 and important residues such as Arg228, influence the mode of substrate binding. Thus, suggesting that the substrate binding pocket of VIM-2 is better defined and allows more stable interactions with the substrates and enhances the catalytic activity. In contrast, VIM-7 substrate binding pocket is more open, allows less stable interactions with substrates is the reason for lower catalytic efficiency for VIM-7 compared to VIM-2.

Paper II: *"Genetic and biochemical characterization of novel metallo-β-lactamase, TMB-1, from an Achromobacter xylosoxidans strain isolated in Tripoli, Libya"*

In paper II, a novel subclass B1 MBL (TMB-1) was identified in *A. xylosoxidans* isolate from Tripoli, Libya. The bla_{TMB-1} gene was embedded in a class 1 integron and located on the chromosome. At amino acid level, TMB-1 was most closely

related to DIM-1 (62%) and GIM-1 (51%). The TMB-1 protein of 245 amino acids possessed all the key motifs of MBLs including the zinc binding residues of B1 MBLs. Determination of the kinetic parameters showed that TMB-1 hydrolyzed all β-lactams with the exception of aztreonam. Overall TMB-1 was most active against penicillins mainly due to high turnover rates (k_{cat} values) compared to cephalosporins and carbapenems. The K_m values were highest for carbapenems.

Paper III: *"Crystal structure of mobile metallo-β-lactamase AIM-1 from Pseudomonas aeruginosa: insights into antibiotic binding and the role of Gln157"*

In paper III, we solved the three dimensional structure of AIM-1 at 1.60 Å, AIM-1-3mol at 1.80 Å, and AIM-1-Gln157Ala mutant at 1.73 Å and AIM-1-Gln157Asn at 1.40 Å resolution. AIM-1 share low level of sequence similarities with other B3 MBLs such as L1, FEZ-1, and BJP-1. The overall structure of AIM-1 forms the characteristic αβ/βα fold and the active site contains two well defined zinc ions with Zn1 tetrahedrally coordinated and Zn2 5-fold (trigonal/square pyramidal) coordinated. Three intermolecular disulphide bonds, Cys32-Cys66, Cys208-Cys213, and Cys256-Cys290 were observed in AIM-1. The active site in AIM-1 is narrow and well-defined and formed by two loops, residue 156-166 and residue 223-230. The three dimensional structure and modelling experiments suggest a narrow and well defined R1 site due to Trp38 and Ile225. Further, a unique Gln157 residue in AIM-1 is projected into the R1 site. The R2 site is slightly positively charged due to Arg300. Moreover, bulky side chains of Thr223 and Ile225 define and influence the R2 site. The AIM-1 structure docked with hydrolysed cefoxitin and QM/MM experiments suggest that the NH2 side chain of Gln157 make interactions with the substrate C10 carbonyl and C8 carboxylate (formed after the nucleophilic attack of β-lactam C8 carbon). Kinetic analysis of AIM-1 Gln157Ala and Gln157Asn shown relatively modest changes compared to the wild-type AIM-1. The effects of mutations were dependent on the substrate and mutation. Structurally, ND2 of Asn157 in AIM-1 Gln157Asn occupies a

similar position to Gln157 NE2 in AIM-1. Also, in the AIM-1 Gln157Ala mutant the position of the main chain is little affected.

Paper IV: "Three dimensional structure of metallo-β-lactamase GIM-1 from *Pseudomonas aeruginosa"*

In paper IV, we solved the three dimensional structure of GIM-1 at 1.60 Å resolution, consisting 3 molecules in the asymmetric unit (Mol A, Mol B, and Mol C). GIM-1 shares similarity to IMP enzymes (39% to 43%), VIM enzymes (28% to 31%), NDM enzymes (28.3% to 28.7%) and SPM-1 (28%) on amino acid level. The overall structure of GIM-1 represents the usual MBL characteristic fold "αβ/βα" with two Zn^{2+} ions at the edge between core "ββ" sheets. The GIM-1 active site has a unique HxHxD motif, (HSHED) where Ser117 and Glu119 are unusual at these positions compared to other B1 subclass MBLs. The Zn1 ion is coordinated with H116, H118, and H196, while the Zn2 ion is coordinated by Asp120, Cys221, and His263, respectively. Both Zn^{2+} ions are linked by same water molecule (W_1) in a tetrahedral coordination. The active site is defined by loop regions (loop 1 and loop 2), which involves many substitutions. The Ile64 and Tyr64 residues along with Asp68 residue increases the flexibility of loop 1. The loop 2 residues Arg224, Trp228, and Tyr233 may collectively increase the flexibility of the loop 2 region. Further, positively charged Arg224 residue projected into the active site, thus interfere the substrate interactions. Comparison with VIM-7 docked ceftazidime data suggest that R1 binding pocket of GIM-1 is open (Ile61, Tyr61, Tyr233 residues) and slightly negatively charged (Asp68). Whereas bulky Trp228 residue blocks the substrate binding R2 binding pocket, and thus make narrower. Further, Arg224 residue gives additional positive charge to the R2 binding pocket and projected into the active site, can interferes the interactions with substrates. Hence, GIM-1 exhibit lower affinity towards bulky positively charged R2 group substrates such as cefepime and ceftazidime.

4. Discussion

MBLs are a large and diverse group of β-lactamases that are now disseminating on mobile genetic elements among clinically important Gram-negative pathogens, limiting treatment options for life-threatening infections [72, 74, 121]. Structurally MBLs share the characteristic overall αβ/βα sandwich and general spectrum of activity towards β-lactams [71]. However, MBLs show diversity with respect to the active site structure, Zn coordination, loops, residues involved in the interaction with substrates, and catalytic efficiency towards different substrates [71, 175]. In this project structural, biochemical, and *in silico* analysis of four different MBLs have been investigated to increase the knowledge and understanding of these differences that could contribute to the future development of a clinical inhibitor of MBLs.

4.1 Subclass B1 MBLs; VIM-7, GIM-1, and TMB-1 (Paper I, II and IV):

Among the three different subclasses of MBLs the B1 subclass is the most studied with respect to the structure and biochemistry [71]. Here we have solved the three dimensional structure of two diverse B1 MBLs, VIM-7 and GIM-1, and used an *in silico* approach to study the interactions of β-lactam substrates with VIM-7 and VIM-2. Further, biochemical characterisation of the substrate spectrum of the novel MBL, TMB-1, was investigated.

Zn coordination and affinity:

The active site of VIM-7 (all three structures) and GIM-1 contains two catalytic Zn^{2+} ions coordinated with the conserved residues of B1 subclass, His116, His118, His196 (Zn1 site) and His196, Asp120, and His263 (Zn2 site). The Zn1 ion in VIM-7, VIM-7-S, and GIM-1 were tetrahedrally coordinated (three His residues and W1) as observed for other B1 subclass MBLs [71]. In contrast, the

Zn1 ion in the VIM-7-Ox structure was trigonal bipyramidally coordinated due to an additional water molecule (W2) as observed for IND-7 [142]. The Zn2 ion in the VIM-7-Ox, VIM-7-S, and GIM-1 structures were coordinated in the usual tetrahedral coordination (Asp120, Cys221, His263 and W1). In contrast, Zn2 in the VIM-7 structure was trigonal bipyramidally coordinated as observed for IND-7 [142] due to an additional water molecule (W3). Further variations in the Zn1-Zn2 distances were observed between the VIM-7 and GIM-1 structures and compared to other B1 MBLs. Overall; this indicates that the coordination geometry of both zinc sites in subclass B1 enzymes is flexible as suggested for other B1 MBLs structures [140, 203].

Oxidation of the Zn2 coordinating residue, Cys221 into a cysteine sulfonate residue (Ocs221) has been observed in different B1 MBL structures such as VIM-2 (PDB id: 1KO2), BcII (PDB id: 2BC2 and 3BC2), and SPM-1 (PDB id: 2FHX) [204]. In the VIM-2 oxidized structure, monozinc BcII, and SPM-1 structure, it was observed that the Zn2 ion is lost [139, 157, 204], suggesting that the loss of Zn2 due to low affinity, might render the Cys221 residue being susceptible for oxidation [204]. Further, the VIM-2 oxidized structure suggested that the oxidation of Cys221 occurred during the crystallization process. The oxidation of the Cys221 residue indicates lower affinity of Zn2 compared to Zn1 and is supported by previous inhibition experiments [177]. In contrast, we observed a mixture of Cys221 with Zn2 and Ocs221 with no Zn2 in the VIM-7-Ox structure. Zn1 and Zn2 affinity variations might be the reason for the loss of the Zn2 ion which has lower affinity compared to Zn1. However, the crystallization process might also have resulted in the observation of a mixture of Cys221 with Zn2 and Ocs221 with no Zn2 in the VIM-7-Ox structure. For GIM-1 structure, we observed the usual Cys221 residue, but in dual conformation.

Loops and residues implicated in the function of VIM-7 and GIM-1:

Several studies on the structures of B1 MBLs have identified loops and residues that are implicated in the activity and specificity of the enzymes (Table 9) [158, 163, 175, 205-209]. It has been suggested that residues 60-66 which form the loop 1 region are important for the binding of substrates/inhibitors in the active site of B1 MBLs [71, 158]. For example, the deletion of loop 1 in CcrA reduced the catalytic efficiencies towards various β-lactam substrates with up to 1500 fold towards benzylpenicillin [163]. In the loop 1 region, a diversity of residues is observed among the B1 MBLs with the exception of Gly63 which is conserved in all B1 MBLs except in VIM-7 (Asp63). Compared to VIM-2 and VIM-4, VIM-7 harbour many substitutions in loop 1 (Lys60Ser, Leu61Phe, Gly62Asp, Asp63Gly and Thr64Ala). In the VIM-7 structures, loop 1 was positioned farther away from the active site than in the native VIM-2 [139], VIM-2-Inhibitor [140], and VIM-4 [141] structures, leading to a more open active site. In addition, the presence of Lys60, Leu61, and Thr64 in loop 1 as well as Pro68 may also increase the flexibility of loop 1.

Table 9: Comparison of residues suggested for kinetic variations between VIM-7, VIM-2, and GIM-1.

	Loop1 (60-66)					**Loop2 (223-242)**		
	60	**61**	**64**	**66**	**218**	**224**	**228**	**233**
VIM-7	Lys	Leu	-	Val	Phe	His	Arg	Asn
VIM-2	Ser	Phe	-	Val	Tyr	Tyr	Arg	Asn
GIM-1	Asn	Ile	Tyr	Leu	Phe	Arg	Trp	Tyr

In VIM-7, Lys60 points away from the active site groove but introduces an additional positive charge contributing to the less negatively surface charge of VIM-7 compared to other B1 MBLs. IMP-1 [79] and NDM-1 [144] contains the

negatively charged residues Glu60 and Asp60, respectively while VIM-2, VIM-4, and BcII (Ser60), and GIM-1 (Asn60) harbour neutral residues.

The Phe61 residue is conserved in all VIMs except VIM-7 and suggested to be important for substrate binding and making hydrophobic interactions with Tyr67 and with the methylene group of the mercaptocarboxylate inhibitor in VIM-2 [140]. Further, in VIM-4 it has been suggested that Phe61 interacts with a citrate ion, involved in the coordination of Zn2 [141]. VIM-7 and GIM-1 harbour Leu61 and Ile61 which in contrast cannot form the hydrophobic (aromatic π-π) interactions with substrates and Tyr67 as in VIM-2. In VIM-7, Leu61 contributes to an enlarged active site groove compared to VIM-2 and VIM-4. The Ile61 for GIM-1 influence the dynamicity of loop 1 and might affect the affinity and activity of GIM-1, as observed for VIM-7. However, the role of Phe61 is debatable as a VIM-2 mutational study show that when Phe61 was substituted with a variety of other amino acids no significant differences in ampicillin MIC was observed suggesting that position 61 is not critical for the function or structure of the enzymes. [209].

Trp64 has been shown to be important in IMP-1 and CcrA where its position and flexibility is modified when an inhibitor is bound into the active site [158]. Further, docking of cefoxitin into the IMP-1 active site suggests that the side chain of Trp64 is displaced (movement of Trp64 NE1 chain) by 4.5 Å and thus comes closer to cefoxitin [158], allowing the Trp64 NE1 make interactions with cefoxitin and trapping it into the active site [79]. In addition, BcII Trp64Ala substitution show increased K_m values compared to the wild type particularly for substrates such as cefoxitin and imipenem [158]. In contrast, GIM-1 possess a Tyr residue with a highly reactive "–OH" group at position 64 that might contribute to the lower affinity of GIM-1 compared to IMP-1, VIM-7, VIM-2, and BcII towards imipenem and cefoxitin compared to other substrates [175, 177, 210]. However, the effect of a role for Trp64 might be enzyme specific as Ala64Trp mutation in VIM-2 did not show a significant effect on the MIC to any substrates [209]

In IMP-1, Pro68 residue is suggested to interact with a succinic acid derivative through hydrophobic interactions [137]. Further, VIM-2 and VIM-4 structures revealed that the main chain carbonyl at position 68 acts as a “second shell” Zn2 ligand by making hydrogen-bonding contact with ND1 of His263 [158, 177, 211]. Although VIM-7 contains Ser68 the hydrogen-bonding interactions and second shell interactions are maintained. The change of a rigid amino acid such as Pro68 to a more flexible amino acid such as Ser68 may increase the flexibility of loop 1 and indirectly have an effect on the activity. However, residue 68 in IMP-1 shown indirect effect on the Zn2 site, and the substitution at this position might have influence on kinetic parameters of MBLs [211]. GIM-1 holds a negatively charged residue Asp68 with amino group at this position, which is unusual at this position (all B1 MBLs have a neutral amino acid), and increases the loop 1 flexibility as observed for VIM-7 (lack of Pro68 residue). Though Asp68 can make the hydrophobic interactions as observed for VIM-7, it gives additional negative charge to the loop 1 region and thus might have an influence in the substrate affinities.

Other active site differences (e.g. residues 218, 224, 228 and 233) which are part of the loop 2 region might also have an impact with respect to the enzymatic functions [158, 175, 177, 205, 207, 209, 211, 212]. Analysis of the VIM-2 structure suggest that the hydroxyl group of Tyr218 are part of a hydrogen-bonding network with Asn70 O, Asp84 OD2, and Arg121 NH1 side chains, important for positioning loop 1 near the active site [139]. Whereas for VIM-7, it was observed that Phe218 (lack of –OH group) cannot make a hydrogen bonding network with Arg121 and Asp84 compared to VIM-2, which is essential for positioning of loop 1 for the affinity and catalytic activity. GIM-1 also harbors Phe218, Arg121, and Asp84 residues at the same positions, respectively and resulted in loss of hydrogen-bonding network with the loop 1 region. This will influence the position of loop 1 and thus have an effect on the active site. A mutational study of IMP-1 Phe218Tyr show that the presence of Tyr218 increase the enzyme activity against cephalosporins with a bulky positively charged C3

substituent (R2), such as ceftazidime [213]. Thus, the presence of Phe218 in VIM-7 and GIM-1 could explain the reduced catalytic activities towards type II cephalosporins.

The hydroxyl group of Tyr224 in VIM-2 take part in another hydrogen-bonding network with Gly232 N, via a water molecule to Asn233 O, and the Zn1 ion coordinating residue His196 ND1 side chains [139]. The VIM-2 structure suggests that this hydrogen-bonding network is important to position the loop 2 region near the active site and thus influence the enzyme activity [139, 175]. In VIM-7, this hydrogen-bonding is disrupted due to His224 which lack a hydroxyl group, and influences the position of residues such as Arg228 and Asn233 in loop 2 that are implicated in substrate interactions [158, 175, 205]. In addition, His224 gives rise to a slightly more positively charged binding pocket for VIM-7 compared to VIM-2, thus influencing the binding pocket and affinity towards positively charged cephalosporins. This is supported by a study on VIM-31 which is different from VIM-2 by two residue substitutions, Tyr224His and His252Arg [214]. VIM-31 exhibit lower catalytic efficiencies compared to VIM-2 supporting a role of the Tyr224His substitution with respect to the overall catalytic efficiency [214].

The hydrogen-bonding network might also be abolished in GIM-1 due to the presence of long, positively charged Arg224 which is positioned slightly away from the active site and cannot interact with Asn233 and His196. A structure of IMP-1 complexed with a mercaptocarboxylate inhibitor suggests that Lys224 interacts with the inhibitor. Further, a Lys224Arg mutant in IMP-1 exhibited higher K_m values compared to the wild type, in particular to cefoxitin (300 times) and imipenem (50 times) [212] and shown reduced over all catalytic activity towards cefoxitin (16 times) and imipenem (1600 times) . It was suggested that Lys224, a positively charged residue, is important for electrostatic interactions with the carboxyl moiety of the substrates, such as the C3 position of imipenem and C4 of cefoxitin [212].

Further, a VIM-2-inhibitor study suggests that loop 2 residues such as Arg228 and Asn233 notably orient their positions to accommodate inhibitors, and influence the enzyme activity [140]. IMP-1 is three residues shorter and lack residue 228 [79]. In GIM-1 residues Trp228 and Tyr233 are part of the loop 2 region. The Trp228 residue in GIM-1 is an aromatic and hydrophobic residue, which moved away from the active site compared to the polar positively charged Arg228 residue in VIM-2 and VIM-7, making the binding pocket bit narrower. Thus, GIM-1 Trp228 residue interfere the interactions with bulky R2 group containing substrates such as ceftazidime, cefoxitin and imipenem.

The Asn233 residue of loop 2 is conserved in most of the B1 MBLs, whereas GIM-1, BlaB, TMB-1, DIM-1, and SPM-1 have Tyr233 [157, 176, 215, 216]. Crystallographic data of B1 MBLs suggests that Asn233 performs backbone functions in substrate binding and catalysis and is part of an oxyanion hole [205, 208]. Further, molecular modelling of substrates into the active site of MBLs suggests that the Asn233 amine side chain can interact with the carboxylate moiety of β-lactams [79, 189, 208, 217]. In addition, nitrocefin hydrolysis by Asn233 mutants of the CcrA enzyme show an increase in K_m values, which suggests that Asn233 play an important role in substrate binding early in the catalytic mechanism [208]. Moreover, mutagenesis experiments on Asn233 in IMP-1 suggests that substitutions for this position influence the kinetic parameters based on the substrates [205]. Both BlaB [218], GIM-1, and DIM-1 [176] exhibit similar catalytic values towards cefoxitin, cefepime, and imipenem indicating that Tyr233 might have an influence in the lower affinity and overall catalytic activity of these MBLs.

In silico experiments:

To support our conclusions regarding the involvement of specific residues in VIM-7, docking studies with ceftazidime (type II cephalosporin with a cyclic positively charged R2 group bound to the C3 carbon) and cefotaxime (type I cephalosporin

with a branched polar R2 group) was done into the active site of VIM-7 and VIM-2. The docking studies suggest that for VIM-7, the positively charged R2 group of ceftazidime make interactions differently compared to VIM-2, involving residues such as Phe61 and Tyr67, together with Arg228, without involvement of the Tyr224 residue. The VIM-7 active site docked with cefotaxime suggest that the R2 group of cefotaxime adopted two different conformations, one such as observed for ceftazidime into VIM-7, and the second conformation showed dominant interactions with His224 and Arg228 residues. The R1 group of ceftazidime and cefotaxime adopted nearly similar conformations, while the interactions involving Phe61, Trp87, His118, and Asp119 in both VIM-2 and VIM-7 structures indicating that the R1 binding pocket is poorly defined.

Our docking results are thus consistent with previous crystallographic investigations of MBLs regarding the specific roles for conserved portions of the (hydrolyzed) β-lactam, namely C8 carboxylate, the C4 carboxylate, and the amide nitrogen (N5), in interactions with the MBL zinc center. These interactions are likely to be common for various β-lactams to different MBLs and thus unlikely to contribute to the variations in the substrate specificities of MBLs. However, the interactions of R1 and R2 substituents of different cephalosporins are different for VIM-2 and VIM-7 and thus influence the specificity. The Leu61 residue in VIM-7 is responsible many orientations of the R1 group compared to Phe61 in VIM-2. However, for R2 groups of cephalosporins, different orientations were observed in VIM-2 and VIM-7, apart from residue 224. Thus, compared to VIM-2, in VIM-7 the loop 1 residue substitutions, residue differences at positions 68 and 218 (loss of hydrogen bonding network), collectively influence the repositioning of loop 1 during the substrate binding. The loop 2 residue Arg228 side chain may be required upon binding of some substrates for proper position of the loop 2 region. The residue substitution at 224 in VIM-7 (His) compared to VIM-2 (Tyr) might be energetically disfavoured and results in loss of hydrogen-bonding network involving positions 224 and 228 through the main chain carbonyl of Ala231, as described in a VIM-2-inhibitor structure complex [140]. Further, the docking

shows that VIM-7 forms less stable substrate interactions due to open and flexible binding pockets and thus allows multiple conformations of the substrates than observed in VIM-2, which form more stable substrate interactions due to narrower substrate binding pockets. Thus, the affinity and overall catalytic activity decreases for VIM-7 compared to VIM-2 towards cephalosporins.

Comparison of substrate binding pockets of GIM-1 with VIM-7 ceftazidime data suggest that the R1 binding pocket is formed by residues Ile61, Tyr64, Phe119, and Tyr233, while the R2 binding pocket is formed by Val223, Arg224, Ser225, and Trp228. The GIM-1 has a more open R1 binding pocket due to a flexible loop 1 (Ile61, Trp64 and Asp68 residues) than observed for VIM-7. Further, the Tyr233 residue pointing outwards to the active site are thus less likely to interact with the R2 group of the β-lactams and enhance the loop 2 flexibility. The R2 binding pocket is flexible due to Arg224 results in loss of hydrogen bonding network as observed for VIM-7. Further, Arg224 residue gives additional positive charge to the active site and is projected into the active site which might interfere and influence some substrate interactions. In contrast, the Trp228 residue defines a part of R2 binding site and acts as a cap; hence the R2 binding pocket is bit narrower.

Biochemical properties of the TMB-1 MBL (paper II):

On amino acid level TMB-1 is most related to DIM-1 (62%) and GIM-1 (52%), and overall TMB-1 exhibit broadly similar kinetic values as DIM-1 [215] and GIM-1 [176]. However, there are some noticeable differences including weak affinity towards meropenem and lower turnover (k_{cat}) values particularly towards cephalosporins and carbapenems. Thus, the overall hydrolysis (k_{cat}/K_m) are lower for cephalosporins and carbapenems. Using a secondary structural comparison with VIM-2 show that a gap in TMB-1 is located just prior to loop 1 and there are several amino acid variations in loop 1. As shown for VIM-7 this might contribute to a more flexible loop 1 and have an impact on the kinetic parameters of TMB-1.

Further, TMB-1 harbour residues in loop 2 such as Tyr233 and positively charged Arg224 residues as in GIM-1 as well as Ser228 which is different to other B1 MBLs. These, loop 2 residues might be involved in the structure of the active site and responsible for the kinetic variations towards cephalosporins as suggested for GIM-1 and VIM-7. However, the three dimensional structure of TMB-1 is required for investigation of the role of these residues.

4.2 Subclass B3 MBL; AIM-1 (Paper III):

The B3 subclass enzymes are mostly chromosomally encoded and reported in environmental bacteria, e.g., L1, FEZ-1, and BJP-1. The *bla*$_{\text{AIM-1}}$ is the first reported B3 subclass from a clinically relevant human pathogen, *P. aeruginosa*. The B3 subclass enzyme structures have the characteristic feature of αβ/βα fold, but different in the loop regions and active site architecture compared to B1 and B2 subclass MBLs. Further, AIM-1 has a unique Gln157 residue which is not observed for other MBLs. Here we solved the three dimensional structure of the B3 MBL AIM-1 at 1.60 Å, AIM-1-3mol at 1.80 Å, AIM-1-Gln157Ala mutant at 1.73 Å, and AIM-1-Gln157Asn at 1.40 Å resolution to investigate the structure and functional relationship towards higher catalytic efficiencies of AIM-1 compared to other B3 subclass MBLs.

Active site and Zn-coordination:

The Zn-coordination of AIM-1 are similar to other B3 MBLs and contains two catalytic Zn^{+2} ions, Zn1 coordinated by His116, His118, and His196 and Zn2 coordinated by Asp120, His121, and His263 [71]. In AIM-1 Zn1 and Zn2 share the same water molecule W1 as observed for other MBLs [79, 97, 168], but the W1 is closer to the OD2 of Asp120 residue compared to other structures [97, 153, 154]. The Zn1 has a tetrahedral coordination and Zn2 has a square pyramidal coordination with an additional water molecule W2 as observed for BJP-1 [154]. An additional water molecule, W3 was found close to the Zn1 ligand

His118. Further, an additional metal ion Ca^{2+} was found in the AIM-1 structure, which is coordinated by the Zn2 ligand His263, Ser221, the B3 MBL conserved residue Tyr293, and a water molecule. In the L1-mercaptocarboxylate inhibitor (MCI) and BJP-1 structures it is shown that a water molecule occupies this place with similar coordination [150, 154]. However, the FEZ-1 structure is different where the side chain of Met266 occupies this position [153].

Overall structure and functionally important residues:

The overall structure of AIM-1 contain the characteristic fold of MBLs (αβ/βα), but exhibits variations to other B3 subclass MBLs such as L1 [97], FEZ-1 [153], and BJP-1 [154] with respect to loop regions and residue substitutions. The N-terminus of AIM-1, starting from Ala28 to Leu45 residues forms a hairpin loop that is different. The N-terminus is shorter for FEZ-1 and BJP-1 in 12 residues length [153, 154]. The BJP-1 complex structure with 4-nitrobenzenesulfonamide suggest that this helix1 (H1) region cover the active site in the native structure and is displaced upon binding of the inhibitor [150, 154]. Further, the loop (residues 277-281) connecting β12 and α6 is shorter in AIM-1. The active site defining loops formed by residues 156-162 connecting α4-β7 and 223-230 connecting β11-α5 are different and results in conformational changes in AIM-1 compared to other B3 subclass MBLs. The loop region connecting α4 to β7 show variations in residues and further contains a unique residue, Gln157 in AIM-1 compared to B3 MBLs [97, 153, 154]. The Gln157 residue is projected into the Zn1 site due to the conformational change and thus interacts with W3 molecule, which is in turn hydrogen-bonded to the bridging water molecule, W1. Hence, the Gln157 influence the size of the active site region. Further, a longer β11-α5 region of AIM-1 of two residues compared to FEZ-1, BJP-1, and three residues compared to L1, is projected across the active site and define the AIM-1 active site. In contrast to other B3 MBLs AIM-1 has three intramolecular disulphide bridges formed between residues Cys256-Cys290 (also found in FEZ-1 and L-1), Cys32-Cys66 and Cys208-Cys213. The Cys256-Cys290 bond links α6-α5

helixes, Cys32-Cys66 bond connects the N-terminus to β1-β3 strands and Cys208-Cys213 bond links β10-β11 strands. Thus, all three disulphide bonds contribute to the stability of AIM-1 structure.

Comparison of substrate binding pockets:

The R1 site of substrate binding and interactions into the active site of B3 MBLs were suggested from the structures of L1, FEZ-1, and BJP-1 in native form and in complex with inhibitors [150, 153, 154, 197, 198, 219, 220]. In L1, the R1 site is formed by Tyr32, Trp38, Phe156, and Ile162, and the C3 carboxylate of substrate interacts with residues Ser221 and Ser223 [150, 219]. In FEZ-1, residues Phe119, Tyr36, Tyr156, and Thr163 which are structurally equivalent define a similar R1 pocket, with additional possibility of interactions between Asp160 and the charged R1 substituents of some substrates [153]. In native BJP-1, although some of these hydrophobic residues Trp38, Tyr151, and Leu162 are conserved, additional bulky amino acids Phe31 and Leu226 restrict the R1 pocket and the affinity for many substrates is reduced [154]. The complex of BJP-1 with 4-nitrobenzenesulfonamide (PDB id: 3M8T) suggest that the Trp31 residue displacement occurs upon inhibitor binding to the R1 site [154]. Less structural information regarding the R2 pocket for B3 MBLs is available, other than for FEZ-1 complexed with D-captopril inhibitor where the side chains of Met266, Tyr293, and the aliphatic Lys297 residues define the R2 pocket suggesting that the D-proline ring of the inhibitor occupies the R2 pocket [153]. To investigate the R1 and R2 pockets of AIM-1 we docked hydrolyzed cefoxitin into the AIM-1 (occupied R1 pocket) and for the analysis of the R2 pocket or C3 substituent R2 group interactions of cephalosporins or carbapenems, we used D-captopril. The docking was stabilized with quantum and molecular mechanics (QM/MM), and compared the FEZ-1: D-captopril structure [153]. In AIM-1, Trp38 and Phe119 are present in the R1 pocket, and further the loop formed by residues 156-162 brings the Gln157 residue into the R1 pocket. The residues Thr223, Ile225, Ala266, and Arg300 define the R2 pocket. In the AIM-1 structure presence of

bulky Thr223 and Ile225 residues side chains might influence the substrate interactions and orientation of R2 substituents. Further, Arg300 gives additional positive charge to the R2 pocket of AIM-1 compared to other B3 MBLs. Thus the R1 pocket of AIM-1 is narrower but better defined and the R2 pocket is narrower with a slightly more positively charge compared to other B3 subclass MBLs. Thus, AIM-1 antibiotic binding pockets are well defined and allows for better interactions and turnover values towards most β-lactams, which might explain the higher catalytic efficiencies of AIM-1 compared to other B3 subclass MBLs.

Role of Gln157 in AIM-1 for substrate specificity:

During the hydrolysis, W1 or the same hydroxide ion in MBLs shared by both Zn2 ions is suggested to act as a nucleophile and lead to oxyanion hole formation [97, 133, 168]. In the B1 MBLs, Asn233 is suggested to form part of the oxyanion hole and stabilize the developed negative charge [205, 206]. Whereas in the B3 MBLs, Tyr228 (L1) or Asn225 (FEZ-1) are suggested to perform this role [97, 221]. However, the effect of residue substitutions at this position is dependent on substrates [178, 179]. Further, Zn1 is thought to polarize the β-lactam carbonyl for addition of W1 [222], but involvement or stabilization of the tetrahedral intermediate by other active site elements has not been demonstrated for MBLs. Hence, the oxyanion hole or tetrahedral intermediate formation in the MBLs hydrolytic mechanism is still a debatable issue as no experimental information is available [175, 205].

AIM-1 docked with hydrolyzed cefoxitin suggests that Gln157 occupies the position as Tyr228 in L1 [97] and Asn225 in FEZ-1 [221]. Hence, the Gln157 NE2 side chain interacts both with the one oxygen of the C8 carboxylate group (derived from addition of W1 to the β-lactam carbonyl) and with the R1 (C10) carbonyl oxygen of hydrolyzed cefoxitin. Thus, Gln157 interacts with the substrate by the C10 carboxyl oxygen, and stabilize the oxyanion hole formed after nucleophilic attack by W1 during hydrolysis. Thus, we hypothesized that the

presence of the unique Gln157 residue was involved in the efficient hydrolytic property of AIM-1 compared to other B3 subclass MBLs. To investigate this, we generated the AIM-1 mutants Gln157Ala and Gln157Asn and solved the three dimensional structures along with the steady-state kinetics data in comparison with wild type AIM-1. The Gln157Asn mutant is still able to interact with the hydrolyzed cefoxitin, whereas for the Gln157Ala mutant the interaction was abolished. Further, enzyme kinetics data of both mutants show that moderate changes in the kinetic parameters compared to the wild type AIM-1. Thus, our kinetic data of mutants did not support an essential role of the Gln157 residue, but the docking data suggest that during the hydrolysis Gln157 NE2 side chain interacts with the substrate.

5. Concluding remarks:

The accelerating dissemination of MBLs will increasingly limit treatment possibilities for healthcare-associated infections by Gram-negative bacteria. Identification of clinically effective inhibitors of these enzymes is thus a clinical problem of growing urgency. MBL inhibitors may also be important for development of improved diagnostic methods that will be important for infection control and to limit the spread of MBL genes among bacterial pathogens. Although, available three dimensional structures of native MBLs, and in complex with substrates or inhibitors have provided information regarding loop regions and important residues role for the function of MBLs, still no inhibitor is available to inhibit the MBLs. Further, obtaining the three dimensional structures of MBLs in complex with inhibitors are less successful in many cases. However, determining the three dimensional structures enables the analysis the interactions of chemical compounds (from online chemical libraries) as inhibitors through *in silico* approaches such as virtual ligand screening (VLS). Hence, determination of an accurate high resolution three dimensional structure is a critical step in the process of structure based drug design. Better knowledge of

the biochemical properties of MBLs, of which structure determination is an important part, will also aid in development of MBL inhibitors.

In our studies we have shown that:

The VIM-7 has a tetra-coordinated Zn2 site, and penta-coordinated (VIM-7-Ox) and tetra-coordinated (VIM-7 and VIM-7-S) Zn1 sites which support the flexibility of metal coordination at the active site. Further, the amino acid substitutions at positions 61, 68, 218, and 224 compared to other VIMs, may collectively influence the flexibility of loop 1 and loop 2 regions suggested to interact with the substrates, and could explain the altered specificities towards cephalosporins. Thus, our VIM-7 structure in comparison with other VIMs has shown that the structural differences between variants of same subclass MBLs can influence the kinetic parameters.

A novel subclass B1 MBL (TMB-1) was identified in *A. xylosoxidans* isolate from Tripoli, Libya. The $bla_{\text{TMB-1}}$ gene was embedded in a class 1 integron and located on the chromosome. Determination of the steady-sate kinetic showed that TMB-1 hydrolyze all β-lactams with the exception of aztreonam. Overall, TMB-1 was most active against penicillins mainly due to high turnover rates (k_{cat} values) compared to cephalosporins and carbapenems. The K_m values were highest for carbapenems.

The AIM-1 structure has three intramolecular disulphide bonds, and the loop regions (residues 156-166) orients differently in AIM-1 compared to other B3 subclass MBLs. The structure and modelling experiments suggest that R1 binding pocket is narrow and better defined, and R2 binding pocket has slightly more positive charge due to the Arg300 residue, compared to other B3 subclass MBLs. Further Gln157 was suggested to interact with the bound substrates and

important for the catalytic activity of AIM-1. However, the Gln157Asn, and Gln157Ala mutants of AIM-1 did not show significant reduction in the catalytic activity.

Lastly, GIM-1 has a more flexible loop 1 and loop 2 regions compared to VIMs and IMP-1. The Tyr64 and Arg224 residues could influence the substrate interactions at the active site. The substrate binding pockets of GIM-1 compared to docked ceftazidime of VIM-7 suggest that the R1 binding pocket is more open and slightly negatively charged (Asp68), and R2 binding pocket is partly narrow (Trp228), and slightly positively charged (Arg224) for GIM-1.

6. References

1. Waksman, S.A. and J.E. Flynn, *History of the word 'antibiotic'.* Journal of the history of medicine and allied sciences, 1973. **28**(3): p. 284-6.
2. Davies, J. and D. Davies, *Origins and evolution of antibiotic resistance.* Microbiology and molecular biology reviews : MMBR, 2010. **74**(3): p. 417-33.
3. Walsh, C., *Molecular mechanisms that confer antibacterial drug resistance.* Nature, 2000. **406**(6797): p. 775-781.
4. Fisher, J.F., S.O. Meroueh, and S. Mobashery, *Bacterial resistance to β-lactam antibiotics: compelling opportunism, compelling opportunity.* Chemical reviews, 2005. **105**(2): p. 395-424.
5. Levy, S.B. and B. Marshall, *Antibacterial resistance worldwide: causes, challenges and responses.* Nature medicine, 2004. **10**(12 Suppl): p. S122-9.
6. Tenover, F.C., *Mechanisms of antimicrobial resistance in bacteria.* American journal of infection control, 2006. **34**(5 Suppl 1): p. S3-10; discussion S64-73.
7. Levy, S.B., *Balancing the drug-resistance equation.* Trends in microbiology, 1994. **2**(10): p. 341-2.
8. *EUCAST Definitive Document E.Def 1.2, May 2000: Terminology relating to methods for the determination of susceptibility of bacteria to antimicrobial agents.* Clinical microbiology and infection: the official publication of the European Society of Clinical Microbiology and Infectious Diseases, 2000. **6**(9): p. 503-8.
9. Allen, H.K., et al., *Call of the wild: antibiotic resistance genes in natural environments.* Nature reviews. Microbiology, 2010. **8**(4): p. 251-9.
10. Sykes, R., *The 2009 Garrod lecture: the evolution of antimicrobial resistance: a Darwinian perspective.* The Journal of antimicrobial chemotherapy, 2010. **65**(9): p. 1842-52.
11. Rowe-Magnus, D.A. and D. Mazel, *Resistance gene capture.* Current opinion in microbiology, 1999. **2**(5): p. 483-8.
12. Jeong, S.H., et al., *Characterization of a new integron containing VIM-2, a metallo-β-lactamase gene cassette, in a clinical isolate of Enterobacter cloacae.* The Journal of antimicrobial chemotherapy, 2003. **51**(2): p. 397-400.
13. Davies, J., *Inactivation of antibiotics and the dissemination of resistance genes.* Science, 1994. **264**(5157): p. 375-82.
14. Toleman, M.A., et al., *blaVIM-7, an evolutionarily distinct metallo-β-lactamase gene in a Pseudomonas aeruginosa isolate from the United States.* Antimicrob Agents Chemother, 2004. **48**(1): p. 329-32.
15. Toleman, M.A., et al., *Genetic characterization of a novel metallo-β-lactamase gene, blaIMP-13, harboured by a novel Tn5051-type transposon disseminating carbapenemase genes in Europe: report from the SENTRY worldwide antimicrobial surveillance programme.* The Journal of antimicrobial chemotherapy, 2003. **52**(4): p. 583-90.

16. Toleman, M.A., P.M. Bennett, and T.R. Walsh, *ISCR elements: novel gene-capturing systems of the 21st century?* Microbiology and molecular biology reviews : MMBR, 2006. **70**(2): p. 296-316.
17. Essack, S.Y., *The development of β-lactam antibiotics in response to the evolution of β-lactamases.* Pharmaceutical Research, 2001. **18**(10): p. 1391-1399.
18. Kumar, A. and H.P. Schweizer, *Bacterial resistance to antibiotics: active efflux and reduced uptake.* Advanced drug delivery reviews, 2005. **57**(10): p. 1486-513.
19. Spratt, B.G., *Resistance to antibiotics mediated by target alterations.* Science, 1994. **264**(5157): p. 388-93.
20. Matagne, A., J. Lamotte-Brasseur, and J.M. Frere, *Catalytic properties of class A β-lactamases: efficiency and diversity.* The Biochemical journal, 1998. **330** p. 581-98.
21. Stein, G.E., *Antimicrobial resistance in the hospital setting: impact, trends, and infection control measures.* Pharmacotherapy, 2005. **25**(10 Pt 2): p. 44S-54S.
22. Nikaido, H., *Molecular basis of bacterial outer membrane permeability revisited.* Microbiology and molecular biology reviews : MMBR, 2003. **67**(4): p. 593-656.
23. Hancock, R.E., *Resistance mechanisms in Pseudomonas aeruginosa and other nonfermentative Gram-negative bacteria.* Clinical infectious diseases : an official publication of the Infectious Diseases Society of America, 1998. **27** (Suppl 1): p. S93-9.
24. Cao, V.T., et al., *Emergence of imipenem resistance in Klebsiella pneumoniae owing to combination of plasmid-mediated CMY-4 and permeability alteration.* The Journal of antimicrobial chemotherapy, 2000. **46**(6): p. 895-900.
25. Masuda, N., et al., *Substrate specificities of MexAB-OprM, MexCD-OprJ, and MexXY-oprM efflux pumps in Pseudomonas aeruginosa.* Antimicrobial agents and chemotherapy, 2000. **44**(12): p. 3322-7.
26. Macheboeuf, P., et al., *Penicillin binding proteins: key players in bacterial cell cycle and drug resistance processes.* FEMS microbiology reviews, 2006. **30**(5): p. 673-91.
27. de Lencastre, H., D. Oliveira, and A. Tomasz, *Antibiotic resistant Staphylococcus aureus: a paradigm of adaptive power.* Current opinion in microbiology, 2007. **10**(5): p. 428-35.
28. Russo, T.A., et al., *Penicillin-binding protein 7/8 contributes to the survival of Acinetobacter baumannii in vitro and in vivo.* The Journal of infectious diseases, 2009. **199**(4): p. 513-21.
29. Zamorano, L., et al., *Differential β-lactam resistance response driven by ampD or dacB (PBP4) inactivation in genetically diverse Pseudomonas aeruginosa strains.* The Journal of antimicrobial chemotherapy, 2010. **65**(7): p. 1540-2.
30. Wright, G.D., *Bacterial resistance to antibiotics: enzymatic degradation and modification.* Advanced drug delivery reviews, 2005. **57**(10): p. 1451-70.

31. Ramirez, M.S. and M.E. Tolmasky, *Aminoglycoside modifying enzymes.* Drug resistance updates : reviews and commentaries in antimicrobial and anticancer chemotherapy, 2010. **13**(6): p. 151-71.
32. Fleming, A., *On the antimicrobial action of cultures of a penicillium with special reference to their use in the isolation of B. influenzae.* British Journal of Experimental Pathology, 1929. **10**: p. 226-236.
33. Chain, E.F., H.W; Hardner, A.D; Heatley, N.G; Jennings, M.A; Orr-Ewing, J; Sanders, A.G, *Penicillin as a chemotherapeutic agent.* The Lancet, 1940. **239**(6104): p. 226-228.
34. Hodgkin, D.C., *The X-ray analysis of the structure of penicillin.* Advancement of science, 1949. **6**(22): p. 85-9.
35. Siu, L.K., *Antibiotics: action and resistance in Gram-negative bacteria.* Journal of microbiology, immunology, and infection = Wei mian yu gan ran za zhi, 2002. **35**(1): p. 1-11.
36. Demain, A.L. and R.P. Elander, *The β-lactam antibiotics: past, present, and future.* Antonie van Leeuwenhoek, 1999. **75**(1-2): p. 5-19.
37. Bryskier, A., *Antimicrobial Agents; Penicillins; Chapter 5: p. 113.*
38. Muniz CC, Z.T., Esquivel GR, Fernandez FJ (7 A.D), *Penicillin and cephalosporin production: A historical perspective.* Revista Latinoamericana de Microbiologia. **49**: p. 88-98.
39. Bryskier, A., *Antimicrobial Agents.* Chapter 7 (Oral Cephalosporins): p. 222-223.
40. Albersschonberg, G., et al., *Structure and Absolute-Configuration of Thienamycin.* Journal of the American Chemical Society, 1978. **100**(20): p. 6491-6499.
41. Kahan, J.S., et al., *Thienamycin, a new β-lactam antibiotic. I. Discovery, taxonomy, isolation and physical properties.* The Journal of antibiotics, 1979. **32**(1): p. 1-12.
42. Weaver, S.S., G.P. Bodey, and B.M. LeBlanc, *Thienamycin: new β-lactam antibiotic with potent broad-spectrum activity.* Antimicrobial agents and chemotherapy, 1979. **15**(4): p. 518-21.
43. Kesado, T., T. Hashizume, and Y. Asahi, *Antibacterial activities of a new stabilized thienamycin, N-formimidoyl thienamycin, in comparison with other antibiotics.* Antimicrobial agents and chemotherapy, 1980. **17**(6): p. 912-7.
44. Hellinger, W.C. and N.S. Brewer, *Carbapenems and monobactams: imipenem, meropenem, and aztreonam.* Mayo Clinic proceedings. Mayo Clinic, 1999. **74**(4): p. 420-34.
45. Nicolau, D.P., *Carbapenems: a potent class of antibiotics.* Expert opinion on pharmacotherapy, 2008. **9**(1): p. 23-37.
46. Bonfiglio, G., G. Russo, and G. Nicoletti, *Recent developments in carbapenems.* Expert opinion on investigational drugs, 2002. **11**(4): p. 529-44.
47. Zhanel, G.G., et al., *Comparative review of the carbapenems.* Drugs, 2007. **67**(7): p. 1027-1052.
48. Paterson, D.L. and D.D. Depestel, *Doripenem.* Clinical infectious diseases : an official publication of the Infectious Diseases Society of America, 2009. **49**(2): p. 291-8.

49. Sykes, R.B., et al., *Monocyclic β-lactam antibiotics produced by bacteria.* Nature, 1981. **291**(5815): p. 489-91.
50. Sykes, R.B. and D.P. Bonner, *Aztreonam: the first monobactam.* The American journal of medicine, 1985. **78**(2A): p. 2-10.
51. Sykes, R.B., W.H. Koster, and D.P. Bonner, *The new monobactams: chemistry and biology.* Journal of clinical pharmacology, 1988. **28**(2): p. 113-9.
52. Todar, K., *Online Text Book of Bacteriology.* p. 2.
53. Mirelman, D., R. Bracha, and N. Sharon, *Penicillin-induced secretion of soluble, uncross-linked peptidoglycan by Micrococcus luteus cells.* Biochemistry, 1974. **13**(24): p. 5045-53.
54. Schleifer, K.H. and O. Kandler, *Peptidoglycan types of bacterial cell walls and their taxonomic implications.* Bacteriological reviews, 1972. **36**(4): p. 407-77.
55. Nanninga, N., *Morphogenesis of Escherichia coli.* Microbiology and molecular biology reviews : MMBR, 1998. **62**(1): p. 110-29.
56. van Heijenoort, J., *Formation of the glycan chains in the synthesis of bacterial peptidoglycan.* Glycobiology, 2001. **11**(3): p. 25r-36r.
57. Massova, I. and S. Mobashery, *Kinship and diversification of bacterial penicillin-binding proteins and β-lactamases.* Antimicrobial agents and chemotherapy, 1998. **42**(1): p. 1-17.
58. Ghuysen, J.M., *Penicillin-binding proteins. Wall peptidoglycan assembly and resistance to penicillin: facts, doubts and hopes.* International journal of antimicrobial agents, 1997. **8**(1): p. 45-60.
59. Ghosh, A.S., C. Chowdhury, and D.E. Nelson, *Physiological functions of D-alanine carboxypeptidases in Escherichia coli.* Trends in microbiology, 2008. **16**(7): p. 309-17.
60. Tipper, D.J. and J.L. Strominger, *Mechanism of action of penicillins: a proposal based on their structural similarity to acyl-D-alanyl-D-alanine.* Proceedings of the National Academy of Sciences of the United States of America, 1965. **54**(4): p. 1133-41.
61. Abraham EP, C.E., *An enzyme from bacteria able to destroy penicillin.* Nature, 1940.
62. Livermore, D.M., *β-Lactamases in laboratory and clinical resistance.* Clinical microbiology reviews, 1995. **8**(4): p. 557-84.
63. Majiduddin, F.K., I.C. Materon, and T.G. Palzkill, *Molecular analysis of β-lactamase structure and function.* International journal of medical microbiology : IJMM, 2002. **292**(2): p. 127-37.
64. Bush, K. and J.F. Fisher, *Epidemiological expansion, structural studies, and clinical challenges of new β-lactamases from Gram-negative bacteria.* Annu Rev Microbiol, 2011. **65**: p. 455-78.
65. Walsh, T.R., et al., *Metallo-β-lactamases: the quiet before the storm?* Clin Microbiol Rev, 2005. **18**(2): p. 306-25.
66. Richmond, M.H. and R.B. Sykes, *The β-lactamases of Gram-negative bacteria and their possible physiological role.* Advances in microbial physiology, 1973. **9**: p. 31-88.

67. Ambler, R.P., *The structure of β-lactamases.* Philosophical transactions of the Royal Society of London. Series B, Biological sciences, 1980. **289**(1036): p. 321-31.
68. Bush, K., G.A. Jacoby, and A.A. Medeiros, *A functional classification scheme for β-lactamases and its correlation with molecular structure.* Antimicrobial agents and chemotherapy, 1995. **39**(6): p. 1211-33.
69. Bush, K. and G.A. Jacoby, *Updated functional classification of β-lactamases.* Antimicrob Agents Chemother, 2010. **54**(3): p. 969-76.
70. Bush, K. and J.F. Fisher, *Epidemiological expansion, structural studies, and clinical challenges of new β-lactamases from Gram-negative bacteria.* Annual review of microbiology, 2011. **65**: p. 455-78.
71. Bebrone, C., *Metallo-β-lactamases (classification, activity, genetic organization, structure, zinc coordination) and their superfamily.* Biochemical pharmacology, 2007. **74**(12): p. 1686-701.
72. Cornaglia, G., H. Giamarellou, and G.M. Rossolini, *Metallo-β-lactamases: a last frontier for β-lactams?* The Lancet infectious diseases, 2011. **11**(5): p. 381-93.
73. Walsh, T.R., *The emergence and implications of metallo-β-lactamases in Gram-negative bacteria.* Clinical microbiology and infection : the official publication of the European Society of Clinical Microbiology and Infectious Diseases, 2005. **11** (Suppl 6): p. 2-9.
74. Walsh, T.R., *Emerging carbapenemases: a global perspective.* International journal of antimicrobial agents, 2010. **36** (Suppl 3): p. S8-14.
75. Felici, A., et al., *An overview of the kinetic parameters of class B β-lactamases.* The Biochemical journal, 1993. **291 (Pt 1)**: p. 151-5.
76. Ganta, S.R., et al., *Approaches to the simultaneous inactivation of metallo- and serine-β-lactamases.* Bioorg Med Chem Lett, 2009. **19**(6): p. 1618-22.
77. Rasmussen, B.A. and K. Bush, *Carbapenem-hydrolyzing β-lactamases.* Antimicrobial agents and chemotherapy, 1997. **41**(2): p. 223-32.
78. Fabiane, S.M., et al., *Crystal structure of the zinc-dependent β-lactamase from Bacillus cereus at 1.9 A resolution: binuclear active site with features of a mononuclear enzyme.* Biochemistry, 1998. **37**(36): p. 12404-11.
79. Concha, N.O., et al., *Crystal structure of the IMP-1 metallo β-lactamase from Pseudomonas aeruginosa and its complex with a mercaptocarboxylate inhibitor: binding determinants of a potent, broad-spectrum inhibitor.* Biochemistry, 2000. **39**(15): p. 4288-98.
80. Daiyasu, H., et al., *Expansion of the zinc metallo-hydrolase family of the β-lactamase fold.* FEBS letters, 2001. **503**(1): p. 1-6.
81. Park, H.S., et al., *Design and evolution of new catalytic activity with an existing protein scaffold.* Science, 2006. **311**(5760): p. 535-8.
82. Lim, H.M., J.J. Pene, and R.W. Shaw, *Cloning, nucleotide sequence, and expression of the Bacillus cereus 5/B/6 β-lactamase II structural gene.* Journal of bacteriology, 1988. **170**(6): p. 2873-8.
83. Rasmussen, B.A., Y. Gluzman, and F.P. Tally, *Cloning and sequencing of the class B β-lactamase gene (ccrA) from Bacteroides fragilis TAL3636.* Antimicrobial agents and chemotherapy, 1990. **34**(8): p. 1590-2.

84. Chen, Y., et al., *β-lactamase genes of the penicillin-susceptible Bacillus anthracis Sterne strain.* Journal of bacteriology, 2003. **185**(3): p. 823-30.
85. Hussain, M., et al., *Cloning and sequencing of the metallothioprotein β-lactamase II gene of Bacillus cereus 569/H in Escherichia coli.* Journal of bacteriology, 1985. **164**(1): p. 223-9.
86. Bellais, S., et al., *Molecular characterization of a carbapenem-hydrolyzing β-lactamase from Chryseobacterium (Flavobacterium) indologenes.* FEMS microbiology letters, 1999. **171**(2): p. 127-32.
87. Bellais, S., et al., *Genetic diversity of carbapenem-hydrolyzing metallo-β-lactamases from Chryseobacterium (Flavobacterium) indologenes.* Antimicrobial agents and chemotherapy, 2000. **44**(11): p. 3028-34.
88. Rossolini, G.M., et al., *Characterization and sequence of the Chryseobacterium (Flavobacterium) meningosepticum carbapenemase: a new molecular class B β-lactamase showing a broad substrate profile.* The Biochemical journal, 1998. **332** p. 145-52.
89. Woodford, N., et al., *Carbapenemases of Chryseobacterium (Flavobacterium) meningosepticum: distribution of blaB and characterization of a novel metallo-β-lactamase gene, blaB3, in the type strain, NCTC 10016.* Antimicrobial agents and chemotherapy, 2000. **44**(6): p. 1448-52.
90. Bellais, S., T. Naas, and P. Nordmann, *Genetic and biochemical characterization of CGB-1, an Ambler class B carbapenem-hydrolyzing β-lactamase from Chryseobacterium gleum.* Antimicrobial agents and chemotherapy, 2002. **46**(9): p. 2791-6.
91. Mammeri, H., S. Bellais, and P. Nordmann, *Chromosome-encoded β-lactamases TUS-1 and MUS-1 from Myroides odoratus and Myroides odoratimimus (formerly Flavobacterium odoratum), new members of the lineage of molecular subclass B1 metalloenzymes.* Antimicrobial agents and chemotherapy, 2002. **46**(11): p. 3561-7.
92. Naas, T., S. Bellais, and P. Nordmann, *Molecular and biochemical characterization of a carbapenem-hydrolysing β-lactamase from Flavobacterium johnsoniae.* The Journal of antimicrobial chemotherapy, 2003. **51**(2): p. 267-73.
93. Massidda, O., G.M. Rossolini, and G. Satta, *The Aeromonas hydrophila cphA gene: molecular heterogeneity among class B metallo-β-lactamases.* Journal of bacteriology, 1991. **173**(15): p. 4611-7.
94. Walsh, T.R., et al., *Nucleotide and amino acid sequences of the metallo-β-lactamase, ImiS, from Aeromonas veronii bv. sobria.* Antimicrobial agents and chemotherapy, 1998. **42**(2): p. 436-9.
95. Yang, Y. and K. Bush, *Biochemical characterization of the carbapenem-hydrolyzing β-lactamase AsbM1 from Aeromonas sobria AER 14M: a member of a novel subgroup of metallo-β-lactamases.* FEMS microbiology letters, 1996. **137**(2-3): p. 193-200.
96. Osano, E., et al., *Molecular characterization of an enterobacterial metallo β-lactamase found in a clinical isolate of Serratia marcescens that shows imipenem resistance.* Antimicrobial agents and chemotherapy, 1994. **38**(1): p. 71-8.

97. Ullah, J.H., et al., *The crystal structure of the L1 metallo-β-lactamase from Stenotrophomonas maltophilia at 1.7 A resolution.* J Mol Biol, 1998. **284**(1): p. 125-36.
98. Boschi, L., et al., *The Legionella (Fluoribacter) gormanii metallo-β-lactamase: a new member of the highly divergent lineage of molecular-subclass B3 β-lactamases.* Antimicrobial agents and chemotherapy, 2000. **44**(6): p. 1538-43.
99. Simm, A.M., et al., *A novel metallo-β-lactamase, Mbl1b, produced by the environmental bacterium Caulobacter crescentus.* FEBS letters, 2001. **509**(3): p. 350-4.
100. Rossolini, G.M., et al., *Metallo-β-lactamase producers in environmental microbiota: new molecular class B enzyme in Janthinobacterium lividum.* Antimicrobial agents and chemotherapy, 2001. **45**(3): p. 837-44.
101. Saavedra, M.J., et al., *Sfh-I, a subclass B2 metallo-β-lactamase from a Serratia fonticola environmental isolate.* Antimicrobial agents and chemotherapy, 2003. **47**(7): p. 2330-3.
102. Yamazoe, K., et al., *Distribution of the cfiA gene among Bacteroides fragilis strains in Japan and relatedness of cfiA to imipenem resistance.* Antimicrobial agents and chemotherapy, 1999. **43**(11): p. 2808-10.
103. Maltezou, H.C., *Metallo-β-lactamases in Gram-negative bacteria: introducing the era of pan-resistance?* International journal of antimicrobial agents, 2009. **33**(5): p. 405 e1-7.
104. Walsh, T.R., et al., *Dissemination of NDM-1 positive bacteria in the New Delhi environment and its implications for human health: an environmental point prevalence study.* The Lancet infectious diseases, 2011. **11**(5): p. 355-62.
105. Wilson, M.E. and L.H. Chen, *NDM-1 and the Role of Travel in Its Dissemination.* Current infectious disease reports, 2012.
106. Watanabe, M., et al., *Transferable imipenem resistance in Pseudomonas aeruginosa.* Antimicrobial agents and chemotherapy, 1991. **35**(1): p. 147-51.
107. Iyobe, S., et al., *Detection of a variant metallo-β-lactamase, IMP-10, from two unrelated strains of Pseudomonas aeruginosa and an alcaligenes xylosoxidans strain.* Antimicrobial agents and chemotherapy, 2002. **46**(6): p. 2014-6.
108. Jeannot, K., et al., *IMP-29, a Novel IMP-Type metallo-β-lactamase in Pseudomonas aeruginosa.* Antimicrobial agents and chemotherapy, 2012. **56**(4): p. 2187-90.
109. Papagiannitsis, C.C., et al., *Characterization of metallo-β-lactamase VIM-27, an A57S mutant of VIM-1 associated with Klebsiella pneumoniae ST147.* Antimicrobial agents and chemotherapy, 2011. **55**(7): p. 3570-2.
110. Yong, D., et al., *Characterization of a new metallo-β-lactamase gene, bla(NDM-1), and a novel erythromycin esterase gene carried on a unique genetic structure in Klebsiella pneumoniae sequence type 14 from India.* Antimicrobial agents and chemotherapy, 2009. **53**(12): p. 5046-54.
111. Espinal, P., et al., *Dissemination of an NDM-2-producing Acinetobacter baumannii clone in an Israeli rehabilitation center.* Antimicrobial agents and chemotherapy, 2011. **55**(11): p. 5396-8.

112. Ghazawi, A., et al., *NDM-2 carbapenemase-producing Acinetobacter baumannii in the United Arab Emirates.* Clinical microbiology and infection : the official publication of the European Society of Clinical Microbiology and Infectious Diseases, 2012. **18**(2): p. E34-6.
113. Kaase, M., et al., *NDM-2 carbapenemase in Acinetobacter baumannii from Egypt.* The Journal of antimicrobial chemotherapy, 2011. **66**(6): p. 1260-2.
114. Nordmann, P., A.E. Boulanger, and L. Poirel, *NDM-4 metallo-β-lactamase with Increased Carbapenemase Activity from Escherichia coli.* Antimicrobial agents and chemotherapy, 2012. **56**(4): p. 2184-6.
115. Poirel, L., et al., *Tn125-Related Acquisition of blaNDM-Like Genes in Acinetobacter baumannii.* Antimicrobial agents and chemotherapy, 2012. **56**(2): p. 1087-9.
116. Rieber, H., et al., *Emergence of metallo-β-lactamases GIM-1 and VIM in multidrug-resistant Pseudomonas aeruginosa in North Rhine-Westphalia, Germany.* The Journal of antimicrobial chemotherapy, 2012.
117. Salabi, A.E., et al., *Genetic and biochemical characterization of a novel metallo-β-lactamase, TMB-1, from a Achromobacter xylosoxidans strain isolated from Tripoli, Libya.* Antimicrobial agents and chemotherapy, 2012.
118. Wachino, J., et al., *SMB-1, a novel subclass B3 metallo-β-lactamase, associated with ISCR1 and a class 1 integron, from a carbapenem-resistant Serratia marcescens clinical isolate.* Antimicrobial agents and chemotherapy, 2011. **55**(11): p. 5143-9.
119. Garau, G., et al., *Update of the standard numbering scheme for class B β-lactamases.* Antimicrobial agents and chemotherapy, 2004. **48**(7): p. 2347-9.
120. Galleni, M., et al., *Standard numbering scheme for class B β-lactamases.* Antimicrobial agents and chemotherapy, 2001. **45**(3): p. 660-3.
121. Cornaglia, G., et al., *Metallo-β-lactamases as emerging resistance determinants in Gram-negative pathogens: open issues.* International journal of antimicrobial agents, 2007. **29**(4): p. 380-8.
122. Toleman, M.A., et al., *Molecular characterization of SPM-1, a novel metallo-β-lactamase isolated in Latin America: report from the SENTRY antimicrobial surveillance programme.* The Journal of antimicrobial chemotherapy, 2002. **50**(5): p. 673-9.
123. Poirel, L., C. Heritier, and P. Nordmann, *Genetic and biochemical characterization of the chromosome-encoded class B β-lactamases from Shewanella livingstonensis (SLB-1) and Shewanella frigidimarina (SFB-1).* The Journal of antimicrobial chemotherapy, 2005. **55**(5): p. 680-5.
124. Walsh, T.R., et al., *Enzyme kinetics and biochemical analysis of ImiS, the metallo-β-lactamase from Aeromonas sobria 163a.* The Journal of antimicrobial chemotherapy, 1996. **37**(3): p. 423-31.
125. Hall, B.G., S.J. Salipante, and M. Barlow, *The metallo-β-lactamases fall into two distinct phylogenetic groups.* Journal of molecular evolution, 2003. **57**(3): p. 249-54.
126. Hall, B.G., S.J. Salipante, and M. Barlow, *Independent origins of subgroup Bl + B2 and subgroup B3 metallo-β-lactamases.* Journal of molecular evolution, 2004. **59**(1): p. 133-41.

127. Garau, G., A.M. Di Guilmi, and B.G. Hall, *Structure-based phylogeny of the metallo-β-lactamases.* Antimicrobial agents and chemotherapy, 2005. **49**(7): p. 2778-84.
128. Avison, M.B., Higgins, C. S., von Heldreich, C. J., Bennett, P. M., Walsh, T. R., *Plasmid location and molecular heterogeneity of the L1 and L2 β-lactamase genes of Stenotrophomonas maltophilia.* Antimicrobial Agents and Chemotherapy, 2001. **45**(2): p. 413-9.
129. Docquier, J.D., et al., *CAU-1, a subclass B3 metallo-β-lactamase of low substrate affinity encoded by an ortholog present in the Caulobacter crescentus chromosome.* Antimicrobial agents and chemotherapy, 2002. **46**(6): p. 1823-30.
130. Stoczko, M., et al., *Postgenomic scan of metallo-β-lactamase homologues in rhizobacteria: identification and characterization of BJP-1, a subclass B3 ortholog from Bradyrhizobium japonicum.* Antimicrobial agents and chemotherapy, 2006. **50**(6): p. 1973-81.
131. Carfi, A., et al., *The 3-D structure of a zinc metallo-β-lactamase from Bacillus cereus reveals a new type of protein fold.* The EMBO journal, 1995. **14**(20): p. 4914-21.
132. Chantalat, L., et al., *Structural effects of the active site mutation cysteine to serine in Bacillus cereus zinc-β-lactamase.* Protein science : a publication of the Protein Society, 2000. **9**(7): p. 1402-6.
133. Concha, N.O., et al., *Crystal structure of the wide-spectrum binuclear zinc β-lactamase from Bacteroides fragilis.* Structure, 1996. **4**(7): p. 823-36.
134. Carfi, A., et al., *X-ray structure of the ZnII β-lactamase from Bacteroides fragilis in an orthorhombic crystal form.* Acta Crystallogr D Biol Crystallogr, 1998. **54**(Pt 1): p. 45-57.
135. Toney, J.H., et al., *Antibiotic sensitization using biphenyl tetrazoles as potent inhibitors of Bacteroides fragilis metallo-β-lactamase.* Chemistry & biology, 1998. **5**(4): p. 185-96.
136. Murphy, T.A., et al., *Biochemical characterization of the acquired metallo-β-lactamase SPM-1 from Pseudomonas aeruginosa.* Antimicrobial agents and chemotherapy, 2003. **47**(2): p. 582-7.
137. Toney, J.H., et al., *Succinic acids as potent inhibitors of plasmid-borne IMP-1 metallo-β-lactamase.* The Journal of biological chemistry, 2001. **276**(34): p. 31913-8.
138. Kurosaki, H., et al., *Probing, inhibition, and crystallographic characterization of metallo-β-lactamase (IMP-1) with fluorescent agents containing dansyl and thiol groups.* ChemMedChem, 2006. **1**(9): p. 969-72.
139. Garcia-Saez, I., et al., *The three-dimensional structure of VIM-2, a Zn-β-lactamase from Pseudomonas aeruginosa in its reduced and oxidised form.* Journal of molecular biology, 2008. **375**(3): p. 604-11.
140. Yamaguchi, Y., et al., *Crystallographic investigation of the inhibition mode of a VIM-2 metallo-β-lactamase from Pseudomonas aeruginosa by a mercaptocarboxylate inhibitor.* Journal of medicinal chemistry, 2007. **50**(26): p. 6647-53.

141. Lassaux, P., et al., *Biochemical and structural characterization of the subclass B1 metallo-β-lactamase VIM-4.* Antimicrobial agents and chemotherapy, 2011. **55**(3): p. 1248-55.
142. Yamaguchi, Y., et al., *Structure of metallo-β-lactamase IND-7 from a Chryseobacterium indologenes clinical isolate at 1.65-A resolution.* Journal of biochemistry, 2010. **147**(6): p. 905-15.
143. Kim, Y., et al., *Structure of apo- and monometalated forms of NDM-1--a highly potent carbapenem-hydrolyzing metallo-β-lactamase.* PloS one, 2011. **6**(9): p. e24621.
144. Zhang, H. and Q. Hao, *Crystal structure of NDM-1 reveals a common β-lactam hydrolysis mechanism.* FASEB journal : official publication of the Federation of American Societies for Experimental Biology, 2011. **25**(8): p. 2574-82.
145. Green, V.L., et al., *Structure of New Delhi metallo-β-lactamase 1 (NDM-1).* Acta crystallographica. Section F, Structural biology and crystallization communications, 2011. **67**(Pt 10): p. 1160-4.
146. King, D. and N. Strynadka, *Crystal structure of New Delhi metallo-β-lactamase reveals molecular basis for antibiotic resistance.* Protein science : a publication of the Protein Society, 2011. **20**(9): p. 1484-91.
147. Garau, G., et al., *A metallo-β-lactamase enzyme in action: crystal structures of the monozinc carbapenemase CphA and its complex with biapenem.* Journal of molecular biology, 2005. **345**(4): p. 785-95.
148. Fonseca, F., et al., *Crystal structure of Serratia fonticola Sfh-I: activation of the nucleophile in mono-zinc metallo-β-lactamases.* Journal of molecular biology, 2011. **411**(5): p. 951-9.
149. Nauton, L., et al., *Structural insights into the design of inhibitors for the L1 metallo-β-lactamase from Stenotrophomonas maltophilia.* Journal of Molecular Biology, 2008. **375**(1): p. 257-269.
150. Spencer, J., et al., *Antibiotic recognition by binuclear metallo-β-lactamases revealed by X-ray crystallography.* Journal of the American Chemical Society, 2005. **127**(41): p. 14439-44.
151. Crisp, J., et al., *Structural basis for the role of Asp-120 in metallo-β-lactamases.* Biochemistry, 2007. **46**(37): p. 10664-74.
152. Lienard, B.M., et al., *Structural basis for the broad-spectrum inhibition of metallo-β-lactamases by thiols.* Organic & biomolecular chemistry, 2008. **6**(13): p. 2282-94.
153. Garcia-Saez, I., et al., *Three-dimensional structure of FEZ-1, a monomeric subclass B3 metallo-β-lactamase from Fluoribacter gormanii, in native form and in complex with D-captopril.* Journal of molecular biology, 2003. **325**(4): p. 651-60.
154. Docquier, J.D., et al., *High-resolution crystal structure of the subclass B3 metallo-β-lactamase BJP-1: rational basis for substrate specificity and interaction with sulfonamides.* Antimicrobial agents and chemotherapy, 2010. **54**(10): p. 4343-51.
155. Wang, Z., et al., *Metallo-β-lactamase: structure and mechanism.* Current opinion in chemical biology, 1999. **3**(5): p. 614-22.

156. Crowder, M.W., J. Spencer, and A.J. Vila, *Metallo-β-lactamases: novel weaponry for antibiotic resistance in bacteria.* Accounts of chemical research, 2006. **39**(10): p. 721-8.
157. Murphy, T.A., et al., *Crystal structure of Pseudomonas aeruginosa SPM-1 provides insights into variable zinc affinity of metallo-β-lactamases.* J Mol Biol, 2006. **357**(3): p. 890-903.
158. Moali, C., et al., *Analysis of the importance of the metallo-β-lactamase active site loop in substrate binding and catalysis.* Chemistry & biology, 2003. **10**(4): p. 319-29.
159. Huntley, J.J., et al., *Role of a solvent-exposed tryptophan in the recognition and binding of antibiotic substrates for a metallo-β-lactamase.* Protein science : a publication of the Protein Society, 2003. **12**(7): p. 1368-75.
160. Garcia-Saez, I., et al., *The 1.5-A structure of Chryseobacterium meningosepticum zinc β-lactamase in complex with the inhibitor, D-captopril.* The Journal of biological chemistry, 2003. **278**(26): p. 23868-73.
161. Scrofani, S.D., et al., *NMR characterization of the metallo-β-lactamase from Bacteroides fragilis and its interaction with a tight-binding inhibitor: role of an active-site loop.* Biochemistry, 1999. **38**(44): p. 14507-14.
162. Huntley, J.J., et al., *Dynamics of the metallo-β-lactamase from Bacteroides fragilis in the presence and absence of a tight-binding inhibitor.* Biochemistry, 2000. **39**(44): p. 13356-64.
163. Yang, Y., et al., *Kinetic properties and metal content of the metallo-β-lactamase CcrA harboring selective amino acid substitutions.* The Journal of biological chemistry, 1999. **274**(22): p. 15706-11.
164. Dal Peraro, M., A.J. Vila, and P. Carloni, *Substrate binding to mononuclear metallo-β-lactamase from Bacillus cereus.* Proteins, 2004. **54**(3): p. 412-23.
165. Fabiane, S.M., et al., *Crystal structure of the zinc-dependent β-lactamase from Bacillus cereus at 1.9 A resolution: binuclear active site with features of a mononuclear enzyme.* Biochemistry, 1998. **37**(36): p. 12404-11.
166. Carenbauer, A.L., et al., *Probing substrate binding to metallo-β-lactamase L1 from Stenotrophomonas maltophilia by using site-directed mutagenesis.* BMC biochemistry, 2002. **3**: p. 4.
167. Heinz, U. and H.W. Adolph, *Metallo-β-lactamases: two binding sites for one catalytic metal ion?* Cellular and molecular life sciences : CMLS, 2004. **61**(22): p. 2827-39.
168. Wang, Z., W. Fast, and S.J. Benkovic, *On the mechanism of the metallo-β-lactamase from Bacteroides fragilis.* Biochemistry, 1999. **38**(31): p. 10013-23.
169. Orellano, E.G., et al., *Spectroscopic characterization of a binuclear metal site in Bacillus cereus β-lactamase II.* Biochemistry, 1998. **37**(28): p. 10173-80.
170. Morán-Barrio J, G.J., Lisa MN, Costello AL, Peraro MD, Carloni P, Bennett B, Tierney DL, Limansky AS, Viale AM, Vila AJ., *The metallo-β-lactamase GOB is a mono-Zn(II) enzyme with a novel active site.* The Journal of biological chemistry, 2007. **282**: p. 18286-18293.
171. Davies, R.B. and E.P. Abraham, *Metal cofactor requirements of β-lactamase II.* The Biochemical journal, 1974. **143**(1): p. 129-35.

172. Hernandez Valladares, M., et al., *Zn(II) dependence of the Aeromonas hydrophila AE036 metallo-β-lactamase activity and stability.* Biochemistry, 1997. **36**(38): p. 11534-41.
173. Robert A. Bonomo and Marcelo E. Tolmasky, G.M.R.a.J.-D.D., *Enzyme-Mediated Resistance to Antibiotics: Mechanisms, Dissemination, and Prospects for Inhibition.* (Chapter 9).
174. Bush, K., *Metallo-β-lactamases: a class apart.* Clin Infect Dis, 1998. **27 Suppl 1**: p. S48-53.
175. Docquier, J.D., et al., *On functional and structural heterogeneity of VIM-type metallo-β-lactamases.* The Journal of antimicrobial chemotherapy, 2003. **51**(2): p. 257-66.
176. Castanheira, M., Toleman, M. A.,Jones, R. N.,Schmidt, F. J.,Walsh, T. R., *Molecular characterization of a β-lactamase gene, bla_{GIM-1}, encoding a new subclass of metallo-β-lactamase.* Antimicrob Agents Chemother, 2004. **48**(12): p. 4654-61.
177. Samuelsen, O., et al., *Kinetic characterization of VIM-7, a divergent member of the VIM metallo-β-lactamase family.* Antimicrob Agents Chemother, 2008. **52**(8): p. 2905-8.
178. Mercuri, P.S., et al., *Probing the specificity of the subclass B3 FEZ-1 metallo-β-lactamase by site-directed mutagenesis.* The Journal of biological chemistry, 2004. **279**(32): p. 33630-8.
179. Carenbauer, A.L., et al., *Probing substrate binding to metallo-β-lactamase L1 from Stenotrophomonas maltophilia by using site-directed mutagenesis.* BMC biochemistry, 2002. **3**: p. 4.
180. Franceschini, N., et al., *Purification and biochemical characterization of the VIM-1 metallo-β-lactamase.* Antimicrobial agents and chemotherapy, 2000. **44**(11): p. 3003-7.
181. Vanhove, M., et al., *Role of Cys221 and Asn116 in the zinc-binding sites of the Aeromonas hydrophila metallo-β-lactamase.* Cellular and molecular life sciences : CMLS, 2003. **60**(11): p. 2501-9.
182. Bounaga, S., et al., *The mechanism of catalysis and the inhibition of the Bacillus cereus zinc-dependent β-lactamase.* The Biochemical journal, 1998. **331 (Pt 3)**: p. 703-11.
183. Olsen, L., et al., *Lactam hydrolysis catalyzed by mononuclear metallo-β-lactamases: A density functional study.* Journal of Physical Chemistry B, 2003. **107**(10): p. 2366-2375.
184. Krauss, M., N. Gresh, and J. Antony, *Binding and hydrolysis of ampicillin in the active site of a zinc lactamase.* Journal of Physical Chemistry B, 2003. **107**(5): p. 1215-1229.
185. Fast, W., Z. Wang, and S.J. Benkovic, *Familial mutations and zinc stoichiometry determine the rate-limiting step of nitrocefin hydrolysis by metallo-β-lactamase from Bacteroides fragilis.* Biochemistry, 2001. **40**(6): p. 1640-50.
186. Paul-Soto, R., et al., *Mono- and binuclear Zn2+-β-lactamase. Role of the conserved cysteine in the catalytic mechanism.* The Journal of biological chemistry, 1999. **274**(19): p. 13242-9.

187. Llarrull, L.I., et al., *Asp-120 locates Zn2 for optimal metallo-β-lactamase activity.* The Journal of biological chemistry, 2007. **282**(25): p. 18276-85.
188. Sharma, N.P., et al., *Mechanistic studies on the mononuclear ZnII-containing metallo-β-lactamase ImiS from Aeromonas sobria.* Biochemistry, 2006. **45**(35): p. 10729-38.
189. Xu, D., D. Xie, and H. Guo, *Catalytic mechanism of class B2 metallo-β-lactamase.* The Journal of biological chemistry, 2006. **281**(13): p. 8740-7.
190. McManus-Munoz, S. and M.W. Crowder, *Kinetic mechanism of metallo-β-lactamase L1 from Stenotrophomonas maltophilia.* Biochemistry, 1999. **38**(5): p. 1547-53.
191. Spencer, J., A.R. Clarke, and T.R. Walsh, *Novel mechanism of hydrolysis of therapeutic β-lactams by Stenotrophomonas maltophilia L1 metallo-β-lactamase.* The Journal of biological chemistry, 2001. **276**(36): p. 33638-44.
192. Miller, L.A., K. Ratnam, and D.J. Payne, *β-lactamase-inhibitor combinations in the 21st century: current agents and new developments.* Current opinion in pharmacology, 2001. **1**(5): p. 451-8.
193. Toney, J.H., *Metallo-β-lactamase inhibitors: could they give old antibacterials new life?* Current opinion in investigational drugs, 2003. **4**(2): p. 115-6.
194. Gonzalez, J.M., et al., *The Zn2 position in metallo-β-lactamases is critical for activity: a study on chimeric metal sites on a conserved protein scaffold.* Journal of molecular biology, 2007. **373**(5): p. 1141-56.
195. Hiraiwa, Y., et al., *Metallo-β-lactamase inhibitory activity of phthalic acid derivatives.* Bioorganic & medicinal chemistry letters, 2009. **19**(17): p. 5162-5.
196. Ishii, Y., et al., *In vitro potentiation of carbapenems with ME1071, a novel metallo-β-lactamase inhibitor, against metallo-β-lactamase- producing Pseudomonas aeruginosa clinical isolates.* Antimicrobial agents and chemotherapy, 2010. **54**(9): p. 3625-9.
197. Lienard, B.M., et al., *Inhibitors of the FEZ-1 metallo-β-lactamase.* Bioorganic & medicinal chemistry letters, 2007. **17**(4): p. 964-8.
198. Lassaux, P., et al., *Mercaptophosphonate compounds as broad-spectrum inhibitors of the metallo-β-lactamases.* Journal of medicinal chemistry, 2010. **53**(13): p. 4862-76.
199. Faridoon, et al., *3-mercapto-1,2,4-triazoles and N-acylated thiosemicarbazides as metallo-β-lactamase inhibitors.* Bioorganic & medicinal chemistry letters, 2012. **22**(1): p. 380-6.
200. Bounaga, S., et al., *Cysteinyl peptide inhibitors of Bacillus cereus zinc β-lactamase.* Bioorganic & medicinal chemistry, 2001. **9**(2): p. 503-10.
201. Sanschagrin, F. and R.C. Levesque, *A specific peptide inhibitor of the class B metallo-β-lactamase L-1 from Stenotrophomonas maltophilia identified using phage display.* The Journal of antimicrobial chemotherapy, 2005. **55**(2): p. 252-5.
202. Sun, Q., et al., *Homo-cysteinyl peptide inhibitors of the L1 metallo-β-lactamase, and SAR as determined by combinatorial library synthesis.* Bioorganic & medicinal chemistry letters, 2006. **16**(19): p. 5169-75.

203. Crowder, M.W., et al., *Characterization of the metal-binding sites of the β-lactamase from Bacteroides fragilis.* Biochemistry, 1996. **35**(37): p. 12126-32.
204. Davies, A.M., et al., *Effect of pH on the active site of an Arg121Cys mutant of the metallo-β-lactamase from Bacillus cereus: implications for the enzyme mechanism.* Biochemistry, 2005. **44**(12): p. 4841-9.
205. Brown, N.G., et al., *Analysis of the functional contributions of Asn233 in metallo-β-lactamase IMP-1.* Antimicrobial agents and chemotherapy, 2011. **55**(12): p. 5696-702.
206. Materon, I.C., et al., *Analysis of the context dependent sequence requirements of active site residues in the metallo-β-lactamase IMP-1.* Journal of molecular biology, 2004. **344**(3): p. 653-63.
207. Oelschlaeger, P. and S.L. Mayo, *Hydroxyl groups in the (β)β sandwich of metallo-β-lactamases favor enzyme activity: a computational protein design study.* Journal of molecular biology, 2005. **350**(3): p. 395-401.
208. Yanchak, M.P., R.A. Taylor, and M.W. Crowder, *Mutational analysis of metallo-β-lactamase CcrA from Bacteroides fragilis.* Biochemistry, 2000. **39**(37): p. 11330-9.
209. Borgianni, L., et al., *Mutational analysis of VIM-2 reveals an essential determinant for metallo-β-lactamase stability and folding.* Antimicrobial agents and chemotherapy, 2010. **54**(8): p. 3197-204.
210. *The CCP4 suite: programs for protein crystallography.* Acta crystallographica. Section D, Biological crystallography, 1994. **50**(Pt 5): p. 760-3.
211. Oelschlaeger, P. and J. Pleiss, *Hydroxyl groups in the ββ sandwich of metallo-β-lactamases favor enzyme activity: Tyr218 and Ser262 pull down the lid.* Journal of molecular biology, 2007. **366**(1): p. 316-29.
212. Haruta, S., et al., *Characterization of the active-site residues asparagine 167 and lysine 161 of the IMP-1 metallo β-lactamase.* FEMS microbiology letters, 2001. **197**(1): p. 85-9.
213. Oelschlaeger, P., S.L. Mayo, and J. Pleiss, *Impact of remote mutations on metallo-β-lactamase substrate specificity: implications for the evolution of antibiotic resistance.* Protein science : a publication of the Protein Society, 2005. **14**(3): p. 765-74.
214. Bogaerts, P., et al., *Detection and characterization of VIM-31, a new variant of VIM-2 with Tyr224His and His252Arg mutations, in a clinical isolate of Enterobacter cloacae.* Antimicrobial agents and chemotherapy, 2012.
215. Poirel, L., et al., *Characterization of DIM-1, an integron-encoded metallo-β-lactamase from a Pseudomonas stutzeri clinical isolate in the Netherlands.* Antimicrobial agents and chemotherapy, 2010. **54**(6): p. 2420-4.
216. El Salabi, A., et al., *Genetic and Biochemical Characterization of a Novel metallo-β-lactamase, TMB-1, from an Achromobacter xylosoxidans Strain Isolated in Tripoli, Libya.* Antimicrobial agents and chemotherapy, 2012. **56**(5): p. 2241-5.
217. Prosperi-Meys, C., et al., *Substrate binding and catalytic mechanism of class B β-lactamases: a molecular modelling study.* Cellular and molecular life sciences : CMLS, 2001. **58**(14): p. 2136-43.

218. Vessillier, S., et al., *Overproduction and biochemical characterization of the Chryseobacterium meningosepticum BlaB metallo-β-lactamase.* Antimicrobial agents and chemotherapy, 2002. **46**(6): p. 1921-7.
219. Nauton, L., et al., *Structural insights into the design of inhibitors for the L1 metallo-β-lactamase from Stenotrophomonas maltophilia.* Journal of molecular biology, 2008. **375**(1): p. 257-69.
220. Yang, K.W. and M.W. Crowder, *Inhibition studies on the metallo-β-lactamase L1 from Stenotrophomonas maltophilia.* Archives of biochemistry and biophysics, 1999. **368**(1): p. 1-6.
221. Garcia-Saez, I., et al., *The 1.5-A structure of Chryseobacterium meningosepticum zinc β-lactamase in complex with the inhibitor, D-captopril.* The Journal of biological chemistry, 2003. **278**(26): p. 23868-73.
222. Page, M.I. and A. Badarau, *The mechanisms of catalysis by metallo β-lactamases.* Bioinorganic chemistry and applications, 2008: p. 576297.

Paper I

Pardha Saradhi Borra, Hanna-Kirsti S. Leiros, Rafi Ahmad, James Spencer, Ingar Leiros, Timothy R. Walsh, Arnfinn Sundsfjord and Ørjan Samuelsen. *Structural and computational investigations of VIM-7: insights into the substrate specificity of VIM metallo-β-lactamases.* J Mol Biol, 2011. 411(1): p. 174-89.

Paper II

Allaaeddin El Salabi, Pardha Saradhi Borra, Mark A. Toleman, Ørjan Samuelsen, and Timothy R. Walsh. *Genetic and biochemical characterization of a novel metallo-β-lactamase, TMB-1, from an Achromobacter xylosoxidans strain isolated in Tripoli, Libya.* Antimicrobial agents and chemotherapy, 2012. 56(5): p. 2241-5.

Paper III

Hanna-Kirsti S. Leiros, Pardha S Borra, Bjørn Olav Brandsdal, Kine Susann Waade Edvardsen, James Spencer, Timothy R. Walsh, and Ørjan Samuelsen. *Crystal structure of the mobile metallo-β-lactamase AIM-1 from Pseudomonas aeruginosa: insights into antibiotic binding and the role of Gln157.* **In Press.**

Paper IV

Pardha Saradhi Borra, Ørjan Samuelsen, Marit Sjo Lorentzen, and Hanna-Kirsti Schrøder Leiros. *Three dimensional structure of the subclass B1 mobile metallo-β-lactamase GIM-1 from Pseudomonas aeruginosa.* **Manuscript is ready.**

ISBN 978-82-7589-356-5